DIFFERENCES BETWEEN ROBIN AND NEUMANN EIGENVALUES ON METRIC GRAPHS

RAM BAND, HOLGER SCHANZ, AND GILAD SOFER

Dedicated to our teacher and mentor, Uzy Smilansky, on the occasion of his 82-nd anniversary.

Abstract. We consider the Laplacian on a metric graph, equipped with Robin (δ-type) vertex condition at some of the graph vertices and Neumann-Kirchhoff condition at all others. The corresponding eigenvalues are called Robin eigenvalues, whereas they are called Neumann eigenvalues if the Neumann-Kirchhoff condition is imposed at all vertices. The sequence of differences between these pairs of eigenvalues is called the Robin-Neumann gap.

We prove that the limiting mean value of this sequence exists and equals a geometric quantity, analogous to the one obtained for planar domains [23]. Moreover, we show that the sequence is uniformly bounded and provide explicit upper and lower bounds. We also study the possible accumulation points of the sequence and relate those to the associated probability distribution of the gaps.

To prove our main results, we prove a local Weyl law, as well as explicit expressions for the second moments of the eigenfunction scattering amplitudes.

1. Introduction

The differences between Robin and Neumann eigenvalues of the Laplacian have been the focus of several recent works. Rudnick, Wigman, and Yesha considered this sequence of Robin-Neumann gaps (RNG) for the Laplacian on bounded planar domains and on the hemisphere [21, 22, 23]. They computed the limiting mean value of this RNG sequence, proved some upper and lower bounds, and an almost sure convergence result. Moreover, they posed stimulating open questions and interesting conjectures – such as the existence of planar domains with unbounded RNG sequence, a lower bound for the RNG in the case of dimension larger than two, and convergence in the case of a billiard with uniformly hyperbolic dynamics.

The RNG sequence was studied by Rivière and Royer for the particular case of metric star graphs in [20], where they considered a non self-adjoint Robin condition at the central vertex of a star graph. They showed that the RNG sequence is bounded and with converging mean value. They also expressed this limiting mean value in terms of an associated probability distribution, and discussed some properties of this distribution. While preparing the current manuscript for submission, we became aware of the work [11], where Bifulco and Kerner prove results of similar nature for metric graphs. In particular, they prove a local Weyl law and use it to express the limiting mean value of the RNG for Schrödinger operators on metric graphs, and extend some results for arbitrary self-adjoint vertex conditions.

In the current paper, we address the analogues of the results in [21, 23] for the case of a metric (quantum) graph. We express the limiting mean value (i.e., Cesàro mean) of the RNG sequence (Theorem 1.3), prove a local Weyl law, and express the second moments of the eigenfunction scattering amplitudes (Theorem 1.4). We also provide lower and upper bounds on the RNG (Theorem 1.7), present the associated probability measure (Theorem 1.8), and use it to study the convergence of subsequences (Proposition 1.11). In doing so, we attempt to answer some of the questions proposed in previous works, and compare the results to the ones obtained for domains and star graphs (see Section 7).

To end this introductory part, we note that the dependence of the spectrum on the boundary conditions in planar domains has long been a topic of interest in physics. For instance, the group of Uzy Smilansky used variations of the boundary conditions as a tool in the study of Gutzwiller's trace formula for quantum billiards [25]. Our teacher Uzy has also inspired the present work, and we would therefore like to dedicate it to his anniversary.

1.1. **Basic definitions and notations.** We consider a metric graph Γ, with $\mathcal{V}$ and $\mathcal{E}$ being its vertex set and edge set respectively. Denoting $E := |\mathcal{E}|$, the edge lengths of Γ are determined by the vector $\vec{\ell} \in \mathbb{R}_+^E$ of positive entries. Each edge $e \in \mathcal{E}$ is identified with the interval $[0, \ell_e]$, so that under the natural identification of vertices connected to the appropriate edges, Γ is a compact metric space. The total length of the graph is denoted by $|\Gamma| := \sum_{e\in\mathcal{E}} \ell_e$. For each vertex $v \in \mathcal{V}$, we denote the set of edges connected to v by $\mathcal{E}_v$, and moreover denote the degree of the vertex v by $\deg(v) := |\mathcal{E}_v|$ (If there are loop edges connected to v, the associated edge is counted twice).

Given a metric graph Γ, we consider the Hilbert space $L^2(\Gamma) := \oplus_{e\in\mathcal{E}} L^2([0, \ell_e])$. We can then define the Neumann-Kirchhoff Laplacian (also known as the *standard* Laplacian) by $H^{(0)} = -\frac{d^2}{dx^2}$ acting on each edge, with domain consisting of all Sobolev functions $f \in W^{2,2}(\Gamma) := \oplus_{e\in\mathcal{E}} W^{2,2}([0, \ell_e])$ which satisfy for all $v \in \mathcal{V}$ the so called "continuity-Kirchhoff" condition:

$$\text{Continuity: } \forall e, e' \in \mathcal{E}_v, \quad f|_e(v) = f|_{e'}(v), \tag{1.1}$$

$$\text{Current conservation (Kirchhoff): } \sum_{e\in\mathcal{E}_v} f'|_e(v) = 0, \tag{1.2}$$

where by convention, all derivatives are taken in the outward direction from the vertex. The operator $H^{(0)}$ is self-adjoint, and its spectrum is infinite, discrete, and bounded from below ([9]). We thus denote the spectrum of $H^{(0)}$ by $\lambda_1 \le \lambda_2 \le ... \nearrow \infty$, with a complete orthonormal set of eigenfunctions $(f_n)_{n=1}^{\infty}$ which can be chosen to be real valued.

Let Γ be a metric graph, initially endowed with the Neumann-Kirchhoff Laplacian, as described above. We introduce a perturbation to our initial operator $H^{(0)}$ by selecting a finite subset of vertices $\mathcal{V}_{\mathcal{R}} \subset \mathcal{V}$, and on this subset of vertices imposing the Robin

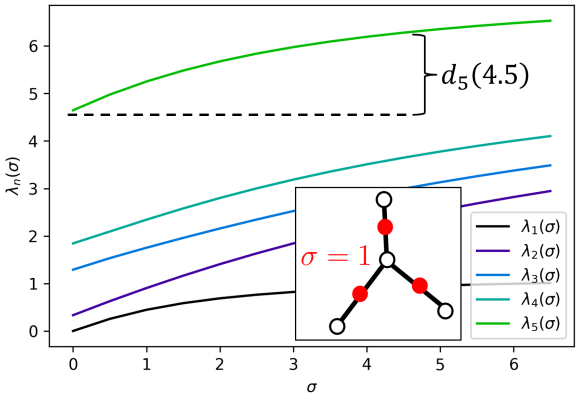

FIGURE 1.1. The Robin eigenvalues $\lambda_n(\sigma)$ for a star graph, along with the Robin-Neumann gap $d_5(4.5)$. The Robin vertices are marked in red.

vertex condition (also known as δ-type vertex condition) with parameter $\sigma \geq 0$:

$$\text{Continuity: } \forall e, e' \in \mathcal{E}_v, \quad f|_e(v) = f|_{e'}(v) =: f(v), \tag{1.3}$$

$$\text{Robin condition: } \sum_{e \in \mathcal{E}_v} f'|_e(v) = \sigma f(v), \tag{1.4}$$

for all $v \in \mathcal{V}_{\mathcal{R}}$. The case $\sigma = 0$ corresponds to the Neumann-Kirchhoff condition; namely, no perturbation at all. Further note that condition (1.4) is the analogue of the Robin boundary condition for manifolds (hence its name).

Remark 1.1. It is also possible to impose the Robin condition at an interior point of an edge. To do so, one simply declares such an interior point as a degree two vertex in $\mathcal{V}$ and adds this vertex to $\mathcal{V}_{\mathcal{R}}$.

We denote the new operator by $H^{(\sigma)}$, and its eigenvalues by $(\lambda_n(\sigma))_{n=1}^{\infty}$. We may also refer to the square roots of the eigenvalues (a.k.a wave numbers), $(k_n(\sigma))_{n=1}^{\infty} := \left(\sqrt{\lambda_n(\sigma)}\right)_{n=1}^{\infty}$, which are well-defined and non-negative since $\mathrm{Spec}\left(H^{(\sigma)}\right) \subset [0, \infty)$ for $\sigma \geq 0$. It is known that the eigenvalues of $H^{(\sigma)}$ are non-decreasing with respect to σ, see [9, prop. 3.1.6]. To quantify this increase, define the *Robin-Neumann gaps* (RNG) by

$$d_n(\sigma) := \lambda_n(\sigma) - \lambda_n(0). \tag{1.5}$$

Recall that the vertex conditions we consider are not the usual Robin and Neumann conditions for manifolds (but rather the δ-type and Neumann-Kirchhoff conditions), and the name RNG serves more as an analogy. The RNG defines an infinite sequence of functions $(d_n(\sigma))_{n=1}^{\infty}$, which measures the increase in the spectrum of $H^{(\sigma)}$ due to the δ perturbation (see Figure 1.1). The current paper focuses on studying the main properties of this sequence.

1.2. **Main results.**

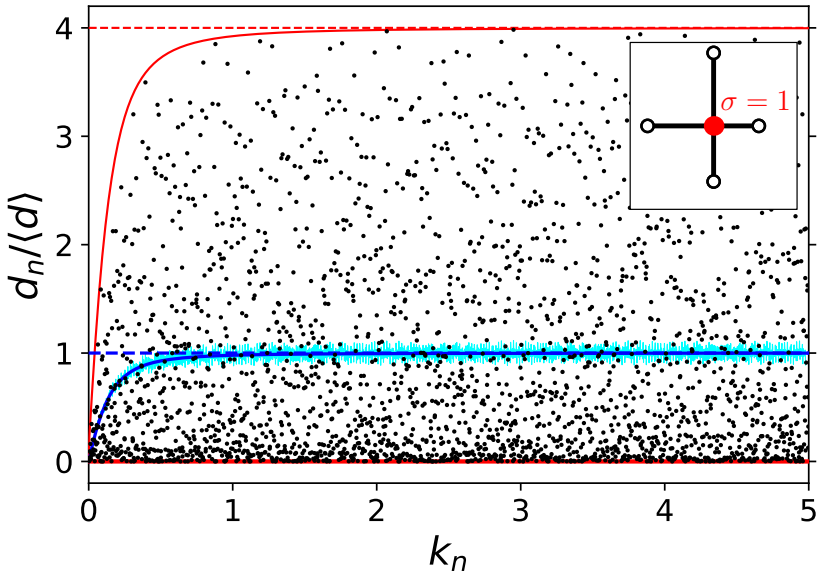

FIGURE 1.2. Scatter plot of the first 2,500 Robin-Neumann gaps for a star graph with four edges and Robin condition at the central vertex, normalized so that $\langle d\rangle_n(\sigma) = 1$. The light blue line is a running average and the blue lines on top of it are the analytic results from Equations (1.7), (A.12). The red dashed line is the first upper bound presented in Equation (1.14), while the solid red line is the finer upper bound appearing in Equation (6.24) (under the star decomposition described in Subsection 6.2).

Definition 1.2. Given a sequence of numbers $(c_n)_{n=1}^{\infty}$, the Cesàro mean (or Cesàro sum) of the sequence is

$$\langle c\rangle_n := \lim_{N\to\infty} \frac{1}{N}\sum_{n=1}^{N} c_n, \tag{1.6}$$

assuming that the limit exists.

The first result concerns the Cesàro mean of the Robin-Neumann gaps:

Theorem 1.3. *The Cesàro mean of the Robin-Neumann gap exists and satisfies*

$$\langle d\rangle_n(\sigma) = \frac{2\sigma}{|\Gamma|}\sum_{v\in\mathcal{V}_{\mathcal{R}}} \frac{1}{\deg(v)}, \tag{1.7}$$

where $|\Gamma|$ *is the total length of the graph and* $\deg(v)$ *is the degree of the vertex* v.

To prove Theorem 1.3, we prove a result which has its own interest – a local Weyl law and expressions for the second moments of the eigenfunction scattering amplitudes:

Theorem 1.4. *Denote by $(f_n)_{n=1}^{\infty}$ the L^2 normalized eigenfunctions of the Neumann-Kirchhoff Laplacian $H^{(0)}$. Then for each vertex $v \in \mathcal{V}$,*

$$\left\langle |f(v)|^2 \right\rangle_n = \frac{2}{\deg(v)\,|\Gamma|}. \tag{1.8}$$

Moreover, expressing these eigenfunctions on each edge $e \in \mathcal{E}$ by

$$f_n|_e(x) = (a_e)_n \exp(\mathrm{i}k_n x) + (a_{\hat{e}})_n \exp(\mathrm{i}k_n(\ell_e - x)), \tag{1.9}$$

we have

$$\forall e \in \mathcal{E}, \quad \left\langle |a_e|^2 \right\rangle_n = \left\langle |a_{\hat{e}}|^2 \right\rangle_n = \frac{1}{2\,|\Gamma|}, \tag{1.10}$$

$$\forall e_1, e_2 \in \mathcal{E}, \text{ such that } e_1 \neq e_2, \quad \left\langle a_{e_1}\overline{a_{e_2}} \right\rangle_n = 0. \tag{1.11}$$

Remark 1.5. The local Weyl law for quantum graphs was recently proven by Borthwick, Harrell and Jones in [13] via heat kernel methods. Afterwards, Bifulco and Kerner had shown that the result may be generalized to Schrödinger operators with arbitrary self-adjoint vertex conditions [11].

Proposition 1.6. *The sequence of functions $(d_n(\sigma))_{n=1}^{\infty}$ is uniformly Lipschitz continuous in $[0,\infty)$. Namely, there exists $C \in \mathbb{R}$ such that*

$$\forall n \in \mathbb{N}, \quad \forall \sigma_1, \sigma_2 \geq 0, \quad |d_n(\sigma_1) - d_n(\sigma_2)| \leq C\,|\sigma_1 - \sigma_2|. \tag{1.12}$$

In particular, the sequence of functions $(d_n(\sigma))_{n=1}^{\infty}$ is uniformly bounded on any compact interval.

Proposition 1.6 is a simple corollary of Lemma 3.1 proven later. With some more effort, it is possible to obtain explicit bounds for the Robin-Neumann gap. In order to do so, we introduce an auxiliary construction.

Let Γ be a metric graph. A *star decomposition* of Γ is a partition of Γ into star graphs, whose central vertices are the vertices of Γ. Such a partition may be described by introducing an auxiliary vertex u_e on each edge $e \in \mathcal{E}$. The vertex u_e may be positioned in the interior of e (so that $\deg(u_e) = 2$), or at its boundary (so that $u_e \in \mathcal{V}$). We denote the set of all such auxiliary vertices connected to v by $\mathcal{U}_v$. Hence, for each $v \in \mathcal{V}$, the associated star subgraph of the partition consists of the central vertex v and all vertices in $\mathcal{U}_v$, together with the corresponding edges. This star subgraph is denoted by $\mathcal{S}_v$, and the edge lengths of this graph are denoted by $\{s_{v,u}\}_{u\in\mathcal{U}_v}$. For example, if an edge e of Γ connects the vertices $v, w \in \mathcal{V}$ and $u_e \in \mathcal{U}_v \cap \mathcal{U}_{v'}$, then $\ell_e = s_{v,u_e} + s_{w,u_e}$. Note that it is also possible to have $s_{v,u_e} = 0$ if the corresponding auxiliary vertex is placed at the boundary of the edge e, such that $u_e = v$. We further denote the total edge length of each star by

$$|\mathcal{S}_v| := \sum_{u\in\mathcal{U}_v} s_{v,u}. \tag{1.13}$$

An example of a star decomposition for a tetrahedron graph can be seen in Figure 1.3.

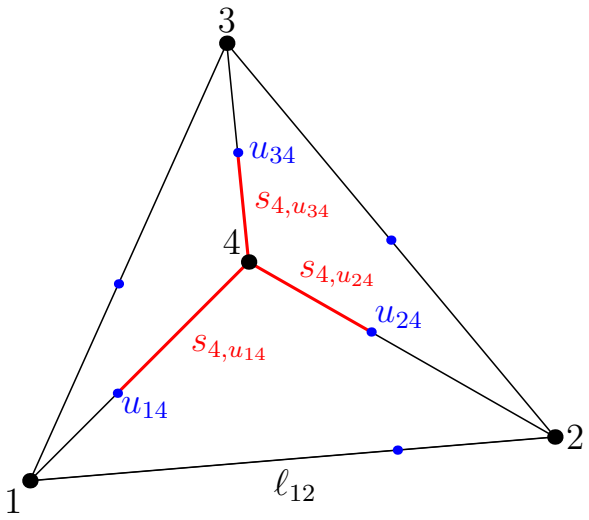

FIGURE 1.3. Star decomposition of a tetrahedron graph. The vertices and edges of the original graph are shown in black. The small blue dots correspond to the auxiliary vertices. The star graph around vertex 4 is highlighted in red.

Theorem 1.7. *For any star decomposition of the metric graph* Γ *and* $\sigma > 0$*:*

$$0 \leq \quad d_n(\sigma) < \tfrac{2\sigma}{\min_{v\in\mathcal{V}_{\mathcal{R}}}|\mathcal{S}_v|}. \tag{1.14}$$

In particular,

$$d_n(\sigma) < \frac{4\sigma}{\ell_{\min}}, \tag{1.15}$$

where $\ell_{\min}$ *is the length of the shortest edge in* Γ*.*

In fact, Proposition 6.3 which appears in the sequel gives a better upper bound than (1.14), but is expressed in a more cumbersome manner. Figure 1.2 demonstrates both the bound (1.14) above (dashed red curve) and the better bound (6.24) in Proposition 6.3 (solid red curve). Note that for a star graph with a single Robin vertex v at its center, the optimal bound in (1.14) is obtained by the star partition which consists of just a single star – the whole graph. For this partition, $|\mathcal{S}_v| = |\Gamma|$ and the upper bound in (1.14) is $\frac{2\sigma}{|\Gamma|}$. See further discussion in Appendix C.

After presenting results about the mean value and bounds of the RNG, we now turn to discuss properties of its value distribution and limit points of its subsequences.

Theorem 1.8. *For* $\sigma > 0$ *define the function*

$$F_\sigma : \mathbb{R} \to [0,1], \tag{1.16}$$

$$F_\sigma(x) := \lim_{N\to\infty} \frac{1}{N} \left|\{n \leq N \ : \ d_n(\sigma) \leq x\}\right|. \tag{1.17}$$

Then F_σ *is a cumulative distribution function whose associated probability measure* μ_σ *is compactly supported on* $\left[0, \frac{4\sigma}{\ell_{\min}}\right]$.

If for all $e, e' \in \mathcal{E}$, $\ell_e/\ell_{e'} \in \mathbb{Q}$ (i.e, the edge lengths are all pairwise rationally dependent), then μ_σ is finitely supported.

Remark 1.9. We conjecture that if not all ratios of edge lengths are rational, then the measure μ_σ is absolutely continuous with respect to the Lebesgue measure. This is further discussed in Remark 5.1 after the proof of the theorem.

Remark 1.10. Theorem 1.8 is similar in spirit to theorem 1.3 in [20], which holds for star graphs with complex Robin parameter.

Interestingly, applying Theorem 1.8 yields information about the possible limit points of the RNG sequence. While for particular values of σ the sequence $(d_n(\sigma))_{n=1}^{\infty}$ does not necessarily converge (as seen in Figure 1.2), we show that there exist subsequences of $(d_n(\sigma))_{n=1}^{\infty}$ which converge uniformly to a linear function.

Proposition 1.11. *There exists a finite collection of compact intervals $(I_j)_{j=1}^N$, such that for every $c \in \bigcup_{j=1}^N I_j$, there exists a subsequence $(d_{n_m}(\sigma))_{m=1}^{\infty}$ which converges to the linear function $c\sigma$ uniformly on any compact subset of $[0,\infty)$. These are the only possible partial limits of $d_n(\sigma)$.*
The intervals $(I_j)_{j=1}^N$ do not depend on the graph edge lengths, as long as the edge lengths are linearly independent over $\mathbb{Q}$.
In the other extreme, if for all $e, e' \in \mathcal{E}$, $\ell_e/\ell_{e'} \in \mathbb{Q}$ then these intervals are in fact degenerate (i.e. consist of a single point).

Remark 1.12. We comment on several possible generalizations of the results above.

(i) For $\sigma < 0$, the operator H_σ has only finitely many negative eigenvalues. Thus, all results except for Theorem 1.7 still hold for $\sigma < 0$ (although the corresponding proofs are slightly more subtle). In addition, the results may be naturally extended for the case where each vertex in $\mathcal{V}_\mathcal{R}$ has its own value of σ (rather than σ being the same at all these vertices). The adaption of the statements is rather straightforward.

(ii) In all results expect for Theorem 1.7, one may replace the Laplacian with a Schrödinger operator $H^{(\sigma)} = -\frac{d^2}{dx^2} + V(x)$, with $V(x) \in L^\infty(\Gamma)$ and the same vertex conditions. This is done in [11] for Theorems 1.3, 1.4.

The structure of the paper is as follows. Section 2 is devoted to introducing several tools which are required for the proofs. The Cesàro mean of the RNG (Theorem 1.3) is computed in Section 3, along with a short proof of Proposition 1.6 as a corollary of Lemma 3.1. The local Weyl law and the expressions of second moments of the scattering amplitudes (Theorem 1.4) which are used in the proof of Theorem 1.3 are proven in Section 4. Section 5 is dedicated to the proofs of Theorem 1.8 and Proposition 1.11; it also contains a discussion of the probability distribution and limit points of the RNG. The explicit bounds on the RNG from Theorem 1.7 are proven in Section 6, along with proof for a better bound. Finally, Section 7 contains a comparison of our results to the analogous statements for domains and star graphs, as well as several open questions.

2. Review of tools and methods for proofs

In this section, we review some existing tools of spectral analysis on metric graphs. These tools are useful in the proofs presented in the following sections.

2.1. **Expressing the Robin-Neumann gap via eigenfunction values.** A main ingredient used in the proofs is the following formula, which relates the RNG to the values that the eigenfunctions attain on the set $\mathcal{V}_R$.

Lemma 2.1. *The RNG is given by*

$$d_n(\sigma) = \sum_{v\in\mathcal{V}_{\mathcal{R}}} \int_0^\sigma \left|f_n^{(t)}(v)\right|^2 dt, \tag{2.1}$$

where $f_n^{(t)}$ is an n^{th} L^2 normalized eigenfunction of $H^{(t)}$.

Remark 2.2. Lemma 2.1 allows us to assume in the forthcoming proofs that the graph contains a single Robin vertex v. The proof for more than one Robin vertex would then follow from the additivity of Equation (2.1).

Proof. We use a straightforward generalization[1] of a formula from [8, prop. 3.1.6],

$$\frac{d\lambda_n(t)}{dt} = \sum_{v\in\mathcal{V}_{\mathcal{R}}} \left|f_n^{(t)}(v)\right|^2. \tag{2.2}$$

The formula holds for all values of t for which $\lambda_n(t)$ is simple.

Note that unless $\lambda_n(t)$ is a multiple eigenvalue for all $t \geq 0$, then the set $D \subset [0,\sigma]$ of t values for which $\lambda_n(t)$ is non-simple must be finite. Indeed, by [9, thm 3.1.2], the eigenvalues $\lambda_n(t)$ are piecewise real analytic in t (see also [8, thms. 3.8, 3.10]). Thus, if $D \subset [0,\sigma]$ was infinite, two of the eigenvalue curves would agree on a set with an accumulation point, and thus agree everywhere. Furthermore, if $\lambda_n(t)$ is a multiple eigenvalue for all t, then by [9, thm 3.1.4], one can locally choose an analytic orthonormal basis for the eigenspace of $\lambda_n(t)$. After doing so, [19, thms 3.23, 3.24] shows that (2.2) also holds for the case where $\lambda_n(t)$ is a multiple eigenvalue for all t, where this time $f_n^{(t)}$ is chosen to be an arbitrary L^2 normalized eigenfunction from the given eigenspace.

Either way, we conclude that (2.2) holds for all but finitely many points in $[0,\sigma]$, and (after possibly dividing the integration along $[0,\sigma]$ into one over finitely many sub-intervals) we get

$$d_n(\sigma) = \lambda_n(\sigma) - \lambda_n(0) = \int_0^\sigma \frac{d\lambda_n(t)}{dt} dt = \sum_{v\in\mathcal{V}_{\mathcal{R}}} \int_0^\sigma \left|f_n^{(t)}(v)\right|^2 dt. \tag{2.3}$$

□

Remark 2.3. When applying Lemma 2.1 in the subsequent sections, we shall conveniently assume that $\lambda_n(t)$ is not a multiple eigenvalue for all t. The proof above shows that this assumption makes no difference, as long as one appropriately chooses the

[1]The original formula refers only to a single Robin vertex. Using additivity arguments in its proof, the more generalized version with multiple Robin vertices follows.

eigenfunction $f_n^{(t)}$ in the degenerate case. To avoid this technicality, we focus on the more standard non-degenerate case.

2.2. **Scattering formalism and the secular equation.** Let $H^{(\sigma)}$ be the operator introduced in Subsection 1.1. An eigenfunction f of $H^{(\sigma)}$, with eigenvalue $k^2 > 0$, can be written on each graph edge $e \in \mathcal{E}$ as

$$f|_e(x) = a_e \exp(\mathrm{i}kx) + a_{\hat{e}} \exp(\mathrm{i}k(\ell_e - x)). \tag{2.4}$$

Thus, f can be described by the vector of coefficients $\vec{a} = (a_1, a_{\hat{1}}, ..., a_E, a_{\hat{E}}) \in \mathbb{C}^{2E}$, which depends on the wave number k. We can think of a_e as representing the amplitude of a (one-dimensional) plane wave propagating along the edge e in the positive direction. Similarly, $a_{\hat{e}}$ represents a wave propagating along the same edge, but in the negative direction. Adopting this physical interpretation, we may consider the graph as a directed graph. Hence, we denote directed edges with opposite directions by e and $\hat{e}$. We follow here the theory which was originally developed by Kottos and Smilanksy in [18, 17].

We note that (2.4) yields straightforwardly that $-f'' = k^2 f$. Yet, the form (2.4) does not guarantee that f satisfies the Robin vertex conditions, as in (1.3),(1.4). In order to satisfy this, one introduces a diagonal edge length matrix $L := \mathrm{diag}(\ell_1, \ell_1, \ell_2, \ell_2, ..., \ell_E, \ell_E)$ and a unitary matrix $S^{(\sigma)} \in U(2E)$. The expression for $S^{(\sigma)}$ depends on the vertex conditions and the wave number k as follows. Given two directed edges e, e', we write that $e \to e'$ at v if the end vertex of e is v and the starting vertex of e' is v. Using this notation, we set (see [15, eq. (3.6)])

$$S^{(\sigma)}_{e'e}(k) = \begin{cases} \frac{2}{\deg(v) + \frac{\mathrm{i}\sigma}{k}} - 1 & e' = \hat{e} \\ \frac{2}{\deg(v) + \frac{\mathrm{i}\sigma}{k}} & e \to e' \text{ at } v \text{ and } e' \neq \hat{e} \\ 0 & \text{Otherwise.} \end{cases} \tag{2.5}$$

After some computation, one gets that

$$\left(I - S^{(\sigma)} \mathrm{e}^{\mathrm{i}kL}\right) \vec{a} = 0, \tag{2.6}$$

whenever $k^2 > 0$ is an eigenvalue of the graph. In such a case, the amplitude vector $\vec{a}$ in (2.6) characterizes the eigenfunction f of that eigenvalue, as in (2.4). This formalism also bears an interesting physical point of view in terms of scattering dynamics on the graph – see [15] for a more elaborate description. We summarize the discussion above with

Theorem 2.4. *([17, 18]) Let $\sigma \geq 0$. $k^2 > 0$ is an eigenvalue of $H^{(\sigma)}$ if and only if*

$$\det\left(I - S^{(\sigma)} \mathrm{e}^{\mathrm{i}kL}\right) = 0. \tag{2.7}$$

The equation $\det\left(I - S\mathrm{e}^{\mathrm{i}kL}\right) = 0$ which describes the graph's eigenvalues is frequently called the *secular equation* (or the *secular function*, when referring just to its left hand side). Theorem 2.4 actually holds for a more general class of vertex conditions (once S is appropriately modified), see [9].

2.3. **The secular manifold.** We now focus on the Neumann-Kirchhoff Laplacian $H^{(0)}$. Motivated by Theorem 2.4, we can define the following function on $\mathbb{R}^E$:

$$\tilde{F}(\vec{x}) = \det\left(I - S\mathrm{e}^{\mathrm{i}\boldsymbol{x}}\right), \tag{2.8}$$

where $\vec{x} := (x_1, ..., x_E)$, $\boldsymbol{x} := \mathrm{diag}(x_1, x_1, ..., x_E, x_E)$, and S here is taken to be $S^{(\sigma)}$ with $\sigma = 0$ (see (2.5)). The function $\tilde{F}$ is clearly 2π-periodic in each of its components, and we can thus consider it as a function F on the torus $\mathbb{T}^E = \mathbb{R}^E/2\pi\mathbb{Z}^E$.

By Theorem 2.4, we conclude that k^2 is an eigenvalue of $H^{(0)}$ if and only if $F(\vec{\kappa}) = 0$, where $\vec{\kappa} := k\vec{\ell} \mod 2\pi = (k\ell_1 \mod 2\pi, ..., k\ell_E \mod 2\pi)$. With this in mind, we consider the following set, first introduced by Barra-Gaspard in [7]:

$$\Sigma := \left\{\vec{\kappa} \in \mathbb{T}^E : F(\vec{\kappa}) = 0\right\}. \tag{2.9}$$

Σ is a compact algebraic subvariety of the torus $\mathbb{T}^E$ known as the secular manifold[2], see [4]. The eigenvalues of $H^{(0)}$ are thus determined by the k values such that the linear torus flow $\phi(k) = (k\ell_1 \mod 2\pi, ..., k\ell_E \mod 2\pi)$ intersects the secular manifold[3]. Moreover, we can define a map between an eigenfunction f of $H^{(0)}$ with eigenvalue k^2 and the corresponding amplitude vector, $\vec{a} \in \ker\left(I - S\mathrm{e}^{\mathrm{i}kL}\right)$, such that the relation (2.4) holds. This map is in fact a linear bijection between the k^2-eigenspace of $H^{(0)}$ and $\ker\left(I - S\mathrm{e}^{\mathrm{i}kL}\right)$, [2, lem. 4.12]. With this in mind, a special emphasis is given to the simple eigenvalues of $H^{(0)}$. To treat those, we define:

$$\Sigma^{\mathrm{reg}} := \left\{\vec{\kappa} \in \Sigma : \dim\ker\left(I - S\mathrm{e}^{\mathrm{i}\boldsymbol{\kappa}}\right) = 1\right\}, \tag{2.10}$$

where $\boldsymbol{\kappa} := \mathrm{diag}(\kappa_1, \kappa_1, ..., \kappa_E, \kappa_E)$. Σ^{reg} is a smooth submanifold of the torus of codimension one ([14, thm 1.1],[4, thm 3.6]). Furthermore, the bijection mentioned above implies that Σ^{reg} classifies the simple eigenvalues of $H^{(0)}$. Namely, $k\vec{\ell} \mod 2\pi \in \Sigma^{\mathrm{reg}}$ if and only if k^2 is a *simple* eigenvalue of $H^{(0)}$. For such $\vec{\kappa} := k\vec{\ell} \mod 2\pi \in \Sigma^{\mathrm{reg}}$, taking $\vec{a}(\vec{\kappa}) \in \ker\left(I - S\mathrm{e}^{\mathrm{i}\boldsymbol{\kappa}}\right)$ provides through (2.4) the unique eigenfunction f (up to scalar multiplication) whose eigenvalue is k^2. Since we know that f can be chosen to be real valued, we get

$$\forall e \in \mathcal{E},\ \ \forall x \in [0, \ell_e], \qquad f|_e(x) = \overline{f|_e(x)} \quad \Leftrightarrow \tag{2.11}$$

$$a_e \exp(\mathrm{i}kx) + a_{\hat{e}} \exp(\mathrm{i}k(\ell_e - x)) = \overline{a_e} \exp(-\mathrm{i}kx) + \overline{a_{\hat{e}}} \exp(-\mathrm{i}k(\ell_e - x)), \tag{2.12}$$

and so

$$a_e = \overline{a_{\hat{e}}} \exp(-\mathrm{i}k\ell_e), \tag{2.13}$$

$$a_{\hat{e}} = \overline{a_e} \exp(-\mathrm{i}k\ell_e). \tag{2.14}$$

Keeping in mind that the coefficients a_e depend on $\vec{\kappa}$ (a dependence which we omitted for brevity), we get

$$a_e(\vec{\kappa}) = \overline{a_{\hat{e}}(\vec{\kappa})} \exp(-\mathrm{i}\vec{\kappa}_e), \tag{2.15}$$

$$a_{\hat{e}}(\vec{\kappa}) = \overline{a_e(\vec{\kappa})} \exp(-\mathrm{i}\vec{\kappa}_e). \tag{2.16}$$

[2]This is a slight misnomer, since generally the secular manifold could have singular points.

[3]To be precise, those k values are the square roots of the eigenvalues of $H^{(0)}$.

We argue that (2.15),(2.16) hold for all $\vec{\kappa} \in \Sigma^{\text{reg}}$, as is explained in the following. Above, (2.15),(2.16) were derived only for those $\vec{\kappa} \in \Sigma^{\text{reg}}$ values for which $\vec{\kappa} := k\vec{\ell}$ mod 2π holds for some value of $k \in \mathbb{R}$. These values form only a countable subset of points in Σ^{reg}. Nevertheless, all points of Σ^{reg} have a similar spectral meaning. Namely, if $\vec{\kappa} \in \Sigma^{\text{reg}}$ is such that there is no $k \in \mathbb{R}$ satisfying $\vec{\kappa} := k\vec{\ell}$ mod 2π, we simply pick a different $\vec{\ell}' \in \mathbb{R}^E$ such that $\vec{\kappa} = k'\vec{\ell}'$ mod 2π for some $k' \in \mathbb{R}$. Doing so means that we consider a graph Γ' with the same connectivity as Γ, but with edge lengths given by $\vec{\ell}'$. We obtain that $(k')^2$ is an eigenvalue of the operator $H^{(0)}$ on this modified graph Γ'. Now, if one repeats the arguments leading to (2.15),(2.16) one concludes that (2.15),(2.16) hold for all $\vec{\kappa} \in \Sigma^{\text{reg}}$.

2.4. **Integrating over the secular manifold – the Barra-Gaspard measure.**

Definition 2.5. ([7, 10, 14]). The *Barra-Gaspard measure* on Σ^{reg} is the Radon probability measure

$$\mathrm{d}\mu_{\vec{\ell}}(\vec{\kappa}) = \frac{\pi}{|\Gamma|} \cdot \frac{1}{(2\pi)^E} \left| \hat{n}\left(\vec{\kappa}\right) \cdot \vec{\ell} \right| \mathrm{d}s, \tag{2.17}$$

where ds is the Lebesgue surface element and $\hat{n}$ is the unit normal to the secular manifold. For a thorough introduction to the Barra-Gaspard measure, see [2, 4, 5, 7, 10, 14].

Remark 2.6. The singular set, $\Sigma \backslash \Sigma^{\text{reg}}$ is of codimension at least one in Σ [14, thm 1.1],[4, thm 3.6], and is thus of measure zero (since $\mu_{\vec{\ell}}$ is a Radon measure). Thus, for the purpose of integration, we may as well extend the Barra-Gaspard measure $\mu_{\vec{\ell}}$ to be defined over the entire secular manifold Σ (by setting it to be zero on the set $\Sigma \backslash \Sigma^{\text{reg}}$). At any rate, the functions we will consider and would like to integrate are only well defined on Σ^{reg}.

The following ergodic theorem will be a main tool in proving our results:

Theorem 2.7. *([7, 10, 14]). Assume that the entries of the vector $\vec{\ell}$ are linearly independent over $\mathbb{Q}$. Let g be a Riemann integrable function on Σ^{reg} (equivalently, g is continuous almost everywhere and bounded). Then:*

$$\langle g \rangle_n := \lim_{N\to\infty} \frac{1}{N} \sum_{n=1}^{N} g\left(k_n \vec{\ell}\right) = \int_{\Sigma^{reg}} g\left(\vec{\kappa}\right) \mathrm{d}\mu_{\vec{\ell}}(\vec{\kappa}) \,. \tag{2.18}$$

Thus, given a Riemann integrable function g on the secular manifold, the ergodic theorem allows us to compute the Cesàro mean of the sequence $\left(g\left(k_n\vec{\ell}\right)\right)_{n=1}^{\infty}$. This will be the main idea behind the proof of Theorem 1.3.

In addition to Theorem 2.7, we will need the following result, which gives further information about the manifold Σ^{reg} and the integration measure $\mu_{\vec{\ell}}$:

Lemma 2.8. *([4, 14]). Let $\vec{\kappa} \in \Sigma^{reg}$ and denote $\boldsymbol{\kappa} := \mathrm{diag}\left(\kappa_1, \kappa_1, ..., \kappa_E, \kappa_E\right)$. Let $\vec{a} \in \ker\left(I - S\mathrm{e}^{\mathrm{i}\boldsymbol{\kappa}}\right)$ be $\mathbb{C}^{2E}$ normalized, i.e., $\|\vec{a}\|_2 = 1$. Let $\hat{n} \in \mathbb{R}^E$ be the unit normal to*

the secular manifold at the point $\vec{\kappa}$.
Then, $\hat{n}$ is given by

$$\forall e \in \mathcal{E}, \qquad \hat{n}_e = |a_e|^2 + |a_{\hat{e}}|^2 . \tag{2.19}$$

3. Proof of Theorem 1.3

To prove Theorem 1.3, we use the following three lemmas. In all lemmas, we denote by $f_n^{(t)}$ the n^{th} L^2 normalized eigenfunction of $H^{(t)}$ (see also Lemma 2.1), and assume for convenience that the associated eigenvalue is simple (confer Remark 2.3).

Lemma 3.1. *For every $v \in \mathcal{V}_R$, the values of $\left|f_n^{(t)}(v)\right|^2$ are uniformly bounded in $n \in \mathbb{N}$ and $t \in \mathbb{R}$.*

Note that Proposition 1.6 now follows as a direct corollary of Lemmas 2.1 and 3.1 (see [26] for further details).

Lemma 3.2. *For $\sigma > 0$ fixed, $\left|f_n^{(t)}(v) - f_n^{(0)}(v)\right| \underset{n\to\infty}{\longrightarrow} 0$ uniformly in $t \in [0,\sigma]$.*

Lemma 3.3. *Fix $\sigma > 0$. Then*

$$\lim_{N\to\infty} \frac{1}{N} \sum_{n=1}^{N} \left|f_n^{(t)}(v)\right|^2 = \lim_{N\to\infty} \frac{1}{N} \sum_{n=1}^{N} \left|f_n^{(0)}(v)\right|^2 , \tag{3.1}$$

where the convergence is uniform in $t \in [0,\sigma]$.

Before proving the lemmas, we use them to prove Theorem 1.3.

Proof of Theorem 1.3. Within this proof, we apply Lemma 2.1, and do so for a single Robin vertex v. The additivity of (2.1) implies that the proof holds for any set $\mathcal{V}_{\mathcal{R}}$ of Robin vertices (see Remark 2.2).

$$\langle d \rangle_n(\sigma) = \lim_{N\to\infty} \frac{1}{N} \sum_{n=1}^{N} d_n(\sigma) \tag{3.2}$$

$$=_{(2.1)} \lim_{N\to\infty} \frac{1}{N} \sum_{n=1}^{N} \int_0^\sigma \left|f_n^{(t)}(v)\right|^2 \mathrm{d}t \tag{3.3}$$

$$= \lim_{N\to\infty} \int_0^\sigma \frac{1}{N} \sum_{n=1}^{N} \left|f_n^{(t)}(v)\right|^2 \mathrm{d}t \tag{3.4}$$

$$= \int_0^\sigma \lim_{N\to\infty} \frac{1}{N} \sum_{n=1}^{N} \left|f_n^{(0)}(v)\right|^2 \mathrm{d}t \tag{3.5}$$

$$= \left\langle \left|f^{(0)}(v)\right|^2 \right\rangle_n \sigma = \frac{2}{\deg(v)\,|\Gamma|}\sigma. \tag{3.6}$$

where we have used Lemma 3.3 when moving to the fourth line, and the local Weyl law (1.8) (which is proven in Section 4) in the last equality. □

Remark 3.4. Appendix A provides an additional approach for deriving the mean value of the RNG and its convergence to the limiting mean value.

Proof of Lemma 3.1. Let $v \in \mathcal{V}_{\mathcal{R}}$. Assume that v is an endpoint of an edge $j \in \mathcal{E}$ and that the parametrization sets v to be at $x = 0$ (This assumption is for convenience, and will be used later as well). Denote by $\widetilde{f}_n^{(t)}$ the eigenfunction of $H^{(t)}$ whose coefficient vector $\vec{a}$ is $\mathbb{C}^{2E}$ normalized, $\|\vec{a}\|_2 = 1$. Since the corresponding eigenvalue is simple, $\widetilde{f}_n^{(t)}$ and $f_n^{(t)}$ equal up to a multiplicative constant. As $f_n^{(t)}$ is L^2 normalized, we can write

$$\left|f_n^{(t)}(0)\right|^2 = \frac{\left|\widetilde{f}_n^{(t)}(0)\right|^2}{\left\|\widetilde{f}_n^{(t)}\right\|_{L^2}^2} = \frac{\left|a_j + a_{\hat{j}}\mathrm{e}^{\mathrm{i}k_n\ell_j}\right|^2}{\sum_{e=1}^{E}\left[\ell_e\left(|a_e|^2 + |a_{\hat{e}}|^2\right) + \frac{2}{k_n}Re\left(a_e\overline{a_{\hat{e}}}\,\mathrm{e}^{-\mathrm{i}k_n\ell_e}\right)\right]}. \tag{3.7}$$

We have used above the expression for $\widetilde{f}_n^{(t)}$ given in (2.4) and performed a straightforward integration to obtain the denominator in (3.7). Note that the coefficients $\{a_e, a_{\hat{e}}\}_{e\in\mathcal{E}}$ depend on n and t, but we suppressed this dependence above for ease of notation. Since a_e and $a_{\hat{e}}$ are all bounded in absolute value by one and $k_n \to \infty$, the right hand side of (3.7) is uniformly bounded in $n \in \mathbb{N}$ and $t \in \mathbb{R}$, which completes the proof (the interested reader may find more details in the proof of lemma 5.2 in [26]). □

Proof of Lemma 3.2. By Theorem 2.4, the eigenvalues of $H^{(t)}$ are $\left(k_n^{(t)}\right)^2$, where $k_n^{(t)}$ are the solutions to the secular equation. Recall that the roots $k_n^{(t)}$, determine the coefficients of the eigenfunction via the (analytic) matrix equation (2.6) and (2.4). It is thus enough to show that as $n \to \infty$, $\left|k_n^{(t)} - k_n^{(0)}\right| \to 0$ uniformly in $t \in [0, \sigma]$.

By Theorem 2.4, $k_n^{(t)}$ are the k values for which $\det\left(I - S^{(t)}\mathrm{e}^{\mathrm{i}kL}\right) = 0$, where

$$S_{j'j}^{(t)} = \begin{cases} \frac{2}{\deg(v)+\frac{\mathrm{i}t}{k}} - 1 & j' = \hat{j} \\ \frac{2}{\deg(v)+\frac{\mathrm{i}t}{k}} & j \to j' \text{ at } v \text{ and } j' \neq \hat{j} \\ 0 & \text{Otherwise,} \end{cases} \tag{3.8}$$

as in (2.5). Denoting $U^{(t)}(k) := S^{(t)}\mathrm{e}^{ikL}$, we get

$$\left\|U^{(t)}(k) - U^{(0)}(k)\right\|_\infty = \left\|\mathrm{e}^{\mathrm{i}kL}\left(S^{(t)} - S^{(0)}\right)\right\|_\infty \leq \frac{2t}{\deg(v)\left|\deg(v) + \frac{\mathrm{i}t}{k}\right|k}, \tag{3.9}$$

and this expression approaches zero uniformly in $t \in [0, \sigma]$ as $k \to \infty$. Since the supremum norm of the difference tends to zero, so does the operator norm of the difference. This means that as $k \to \infty$, the eigenvalues of $U^{(t)}(k)$ converge to those of $U^{(0)}(k)$ uniformly in $t \in [0, \sigma]$. Denote the eigenvalues of the unitary matrix $U^{(t)}(k)$ by $\left(\mathrm{e}^{i\theta_m^{(t)}(k)}\right)_{m=1}^{2E}$, so that the eigenphases $\left(\theta_m^{(t)}(k)\right)_{m=1}^{2E}$ are the lifts of these eigenvalues from S^1 to the universal cover $\mathbb{R}$. By Theorem 2.4, $k^2 > 0$ is an eigenvalue of $H^{(t)}$ if and only if $\theta_m^{(t)}(k) \in 2\pi\mathbb{Z}$ for some m. Denote by $\left(k_n^{(t)}\right)_{n=1}^{\infty}$ the k values for which this happens (these are exactly the zeros of the secular function $\det\left(I - S^{(t)}\mathrm{e}^{\mathrm{i}kL}\right)$).

We know that $\left(\theta_m^{(t)}(k)\right)_{m=1}^{2E}$ increase monotonically with k at a rate which is bounded from below by some $c>0$, and that $k_n^{(0)} < k_n^{(t)}$ for all n, [12, lem. 4.5]. Then by applying the mean value theorem, we get

$$\theta_m^{(0)}\left(k_n^{(0)}\right) = \theta_m^{(t)}\left(k_n^{(t)}\right) \geq \theta_m^{(t)}\left(k_n^{(0)}\right) + c\left(k_n^{(t)} - k_n^{(0)}\right) \tag{3.10}$$

$$\Rightarrow \; k_n^{(t)} - k_n^{(0)} \leq \frac{1}{c}\left(\theta_m^{(0)}\left(k_n^{(0)}\right) - \theta_m^{(t)}\left(k_n^{(0)}\right)\right). \tag{3.11}$$

As $n\to\infty$ (which is equivalent to $k\to\infty$), we know that $\theta_m^{(0)}\left(k_n^{(0)}\right) - \theta_m^{(t)}\left(k_n^{(0)}\right) \longrightarrow 0$ uniformly in $t\in[0,\sigma]$ (as argued in (3.9)). Therefore, we conclude that as $n\to\infty$, $\left|k_n^{(t)} - k_n^{(0)}\right| \to 0$ uniformly in $t\in[0,\sigma]$. This completes the proof. □

Proof of Lemma 3.3. We first note that for $t=0$, $\left\langle \left|f^{(0)}(v)\right|^2 \right\rangle_n$ exists by the local Weyl law in Theorem 1.4. We denote this mean value by C for brevity. For $t\neq 0$, we wish to show that $\left\langle \left|f^{(t)}(v)\right|^2 \right\rangle_n$ exists as well, that it equals the same constant C, and that the convergence is uniform with $t\in[0,\sigma]$. Writing

$$\frac{1}{N}\sum_{n=1}^{N}\left|f_n^{(t)}\right|^2 = \frac{1}{N}\sum_{n=1}^{N}\left|f_n^{(0)}\right|^2 + \frac{1}{N}\sum_{n=1}^{N}\left(\left|f_n^{(t)}\right|^2 - \left|f_n^{(0)}\right|^2\right), \tag{3.12}$$

we have that as $N\to\infty$, the first term converges to C, and we claim that the second term converges to zero uniformly with $t\in[0,\sigma]$. It is enough to show that the expression $\left|f_n^{(t)}\right|^2 - \left|f_n^{(0)}\right|^2$ (without the average) converges uniformly to zero.

Recall by Lemma 3.1 that the values of $\left|f_n^{(t)}(v)\right|^2$ are all uniformly bounded in $t\in\mathbb{R}$ by some $M>0$. Hence,

$$\left|\left|f_n^{(t)}(v)\right|^2 - \left|f_n^{(0)}(v)\right|^2\right| = \left|f_n^{(t)}(v) - f_n^{(0)}(v)\right| \cdot \left|f_n^{(t)}(v) + f_n^{(0)}(v)\right| \tag{3.13}$$

$$\leq 2M\left|f_n^{(t)}(v) - f_n^{(0)}(v)\right| \to 0. \tag{3.14}$$

This convergence is uniform with $t\in[0,\sigma]$, since $\left|f_n^{(t)} - f_n^{(0)}\right| \underset{n\to\infty}{\to} 0$ uniformly by Lemma 3.2, finishing the proof. □

4. Proof of Theorem 1.4

All statements in this section are proven under the following assumption:

Assumption 4.1. *The edge lengths of the graph are linearly independent over* $\mathbb{Q}$.

This assumption allows to conveniently apply Theorem 2.7 in all proofs of the current and the next section. Nevertheless, all the statements are valid even without this assumption. Indeed, in Appendix B we use a simple continuity argument to show that the assumption can be omitted.

In the course of proving Theorem 1.4, we first express the second moments of the eigenfunction scattering amplitudes in two separate lemmas, and then use these expressions to prove the local Weyl law.

Lemma 4.2. *Assume that the eigenfunction scattering amplitudes are $\mathbb{C}^{2E}$ normalized, i.e., $\|\vec{a}\|_2 = 1$. The following holds for all $j \in \mathcal{E}$:*

$$\left\langle \frac{|a_j|^2}{\sum_{e=1}^{E} \ell_e \left(|a_e|^2 + |a_{\hat{e}}|^2\right)} \right\rangle_n = \left\langle \frac{|a_{\hat{j}}|^2}{\sum_{e=1}^{E} \ell_e \left(|a_e|^2 + |a_{\hat{e}}|^2\right)} \right\rangle_n = \frac{1}{2\,|\Gamma|}, \tag{4.1}$$

where the n-dependence of the amplitudes, $(a_j)_n$, is as given in (1.9).

Proof. In order to express the mean value in the left hand side of (4.1), we apply the ergodic theorem (Theorem 2.7) for the function

$$g_j\left(\vec{\kappa}\right) := \frac{|a_j(\vec{\kappa})|^2}{\sum_{e=1}^{E} \ell_e \left(|a_e(\vec{\kappa})|^2 + |a_{\hat{e}}(\vec{\kappa})|^2\right)}, \tag{4.2}$$

where $\vec{a}(\vec{\kappa}) \in \ker\left(I - S\mathrm{e}^{\mathrm{i}\boldsymbol{\kappa}}\right)$ and $\boldsymbol{\kappa} := \mathrm{diag}\left(\kappa_1, \kappa_1, ..., \kappa_E, \kappa_E\right)$. Furthermore, $\vec{a}(\vec{\kappa})$ is a $\mathbb{C}^{2E}$ normalized vector which is chosen as described in Section 2.3 and satisfies (2.15),(2.16). Applying (2.18) from the ergodic theorem gives

$$\langle g_j \rangle_n = \int_{\Sigma^{\mathrm{reg}}} g_j\left(\vec{\kappa}\right) \mathrm{d}\mu_{\vec{\ell}}(\vec{\kappa}), \tag{4.3}$$

where $\left(g_j\right)_n := g_j\left(k_n\vec{\ell}\right)$ and $\left(a_j\right)_n = a_j\left(k_n\vec{\ell}\right)$. We may indeed apply the ergodic theorem, since $|a_j(\vec{\kappa})|^2$ are real analytic functions on Σ^{reg} (see proof of lemma 4.25 in [2]) and the denominator of (1.9) is bounded from below by a positive number, and so g_j is Riemann integrable. We thus get that the mean values in (4.1) are well defined. By (2.15), we further see that $g_j = g_{\hat{j}}$ and conclude

$$\left\langle \frac{|a_j|^2}{\sum_{e=1}^{E} \ell_e \left(|a_e|^2 + |a_{\hat{e}}|^2\right)} \right\rangle_n = \left\langle \frac{|a_{\hat{j}}|^2}{\sum_{e=1}^{E} \ell_e \left(|a_e|^2 + |a_{\hat{e}}|^2\right)} \right\rangle_n. \tag{4.4}$$

This proves the first equality in the lemma, and all that remains is to show that both terms above are equal to $\frac{1}{2|\Gamma|}$. We do so by proving that

$$\left\langle \frac{|a_j|^2 + |a_{\hat{j}}|^2}{\sum_{e=1}^{E} \ell_e \left(|a_e|^2 + |a_{\hat{e}}|^2\right)} \right\rangle_n = \frac{1}{|\Gamma|}. \tag{4.5}$$

We calculate,

$$\left\langle \frac{|a_j|^2 + |a_{\hat{j}}|^2}{\sum_{e=1}^{E} \ell_e \left(|a_e|^2 + |a_{\hat{e}}|^2\right)} \right\rangle_n = \left\langle \frac{\hat{n}_j}{\sum_{e=1}^{E} \ell_e \hat{n}_e} \right\rangle_n = \tag{4.6}$$

$$= \int_{\Sigma^{\mathrm{reg}}} \frac{\hat{n}_j}{\sum_{e=1}^{E} \ell_e \hat{n}_e} \mathrm{d}\mu_{\vec{\ell}} = \frac{\pi}{|\Gamma|} \cdot \frac{1}{(2\pi)^E} \int_{\Sigma} \hat{n}_j \mathrm{d}s, \tag{4.7}$$

where the first equality follows from the expression of the unit normal to Σ^{reg}, (2.19), the second equality is (2.18) in the ergodic theorem, and the third is by the definition of the Barra-Gaspard measure (2.17) and Remark 2.6. Hence, (4.5) is equivalent to showing that $\int_\Sigma \hat{n}_j \mathrm{d}s = 2\,(2\pi)^{E-1}$, which is what we prove next.

The given integral is exactly the surface integral of the vector field $\frac{\partial}{\partial x_j}$ over the secular manifold, Σ. We consider the projection $\pi_j : \Sigma \to (\mathbb{R}/2\pi\mathbb{Z})^{E-1}$, which is defined by omitting the j^{th} coordinate of $\vec{\kappa}$. The proof of proposition 3.1 in [14] shows that this projection is a two to one map. Namely, $\left|\pi_j^{-1}(\vec{x})\right| = 2$ for all $\vec{x} \in (\mathbb{R}/2\pi\mathbb{Z})^{E-1}$. Since the surface integral of $\frac{\partial}{\partial x_j}$ is invariant under this projection, we get that the given integral is equal to twice the flux of the vector field $\frac{\partial}{\partial x_j}$ through the j^{th} face of the torus:

$$\int_\Sigma \hat{n}_j \mathrm{d}s = 2\int_{(\mathbb{R}/2\pi\mathbb{Z})^{E-1}} 1\,\mathrm{d}s = 2\,\mathrm{vol}\left((\mathbb{R}/2\pi\mathbb{Z})^{E-1}\right) = 2\,(2\pi)^{E-1}\,, \tag{4.8}$$

as required. □

Lemma 4.3. *Assume that the eigenfunction scattering amplitudes are $\mathbb{C}^{2E}$ normalized, i.e., $\|\vec{a}\|_2 = 1$. The following holds for all $i, j \in \mathcal{E}$, $i \neq j$:*

$$\left\langle \frac{a_i \overline{a_j}}{\sum_{e=1}^{E} \ell_e \left(|a_e|^2 + |a_{\hat{e}}|^2\right)} \right\rangle_n = 0, \tag{4.9}$$

where the n-dependence of the amplitudes, $(a_j)_n$, is as given in (1.9).

Proof. By the ergodic theorem (Theorem 2.7), combined with Remark 2.6, we have that

$$\langle g \rangle_n = \int_{\Sigma^{\mathrm{reg}}} g \mathrm{d}\mu_{\vec{\ell}} = \int_\Sigma g \mathrm{d}\mu_{\vec{\ell}}. \tag{4.10}$$

We now refer to [5, thm. 4.10], which gives an alternative method for integrating functions over Σ:

$$\int_\Sigma g \mathrm{d}\mu_{\vec{\ell}} = \int_{\mathbb{T}^E} \sum_{m=1}^{2E} g\left(\vec{\kappa} - \theta_m \cdot \vec{1}\right) \frac{\left(\vec{a}^{(m)}\right)^* L \vec{a}^{(m)}}{\mathrm{tr}(L)} \frac{\mathrm{d}\vec{\kappa}}{(2\pi)^E}, \tag{4.11}$$

where $(\mathrm{e}^{\mathrm{i}\theta_m(\vec{\kappa})})_{m=1}^{2E}$ are the eigenvalues of the unitary matrix $S\mathrm{e}^{\mathrm{i}\boldsymbol{\kappa}}$, $(\vec{a}^{(m)}(\vec{\kappa}))_{m=1}^{2E}$ are its $\mathbb{C}^{2E}$ normalized eigenvectors, and $\vec{1} = (1, \ldots, 1)$. Equation (4.11) is useful, as it allows to replace integration over the secular manifold with integration over the whole torus, if the spectral decomposition of $S\mathrm{e}^{\mathrm{i}\boldsymbol{\kappa}}$ is known.

Next, we apply (4.11) for the function

$$g\left(\vec{\kappa}\right) := \frac{a_i \overline{a_j}}{\sum_{e=1}^{E} \ell_e \left(|a_e|^2 + |a_{\hat{e}}|^2\right)}, \tag{4.12}$$

noting that the vector $\vec{a}(\vec{\kappa})$ which appears in g (and in the statement of the lemma) is one of the eigenvectors $\vec{a}^{(n)}$ of the unitary matrix $S\mathrm{e}^{\mathrm{i}\boldsymbol{\kappa}}$ (in particular it is an eigenvector which corresponds to the eigenvalue 1). As a matter of fact, the set of eigenvectors $\left\{\vec{a}^{(m)}\right\}_{m=1}^{2E}$ of $S\mathrm{e}^{\mathrm{i}\boldsymbol{\kappa}}$ is exactly $\left\{\vec{a}(\vec{\kappa} - \theta_i \cdot \vec{1})\right\}_{i=1}^{2E}$ (up to possible reordering, which we

do not care about here). We further observe that $\mathrm{tr}(L) = 2\left|\Gamma\right|$ and $\left(\vec{a}^{(m)}\right)^* L\vec{a}^{(m)} = \sum_{e=1}^{E}\ell_e\left(\left|a_e^{(m)}\right|^2 + \left|a_{\hat{e}}^{(m)}\right|^2\right)$. Using all of the above, we get

$$\left\langle \frac{a_i\overline{a_j}}{\sum_{e=1}^{E}\ell_e\left(\left|a_e\right|^2+\left|a_{\hat{e}}\right|^2\right)}\right\rangle_n = \frac{1}{2\left|\Gamma\right|(2\pi)^E}\int_{\mathbb{T}^E}\sum_{n=1}^{2E} a_i\left(\vec{\kappa}-\theta_n\right)\overline{a_j}\left(\vec{\kappa}-\theta_n\right)\mathrm{d}\vec{\kappa}. \tag{4.13}$$

$$= \frac{1}{2\left|\Gamma\right|(2\pi)^E}\int_{\mathbb{T}^E}\sum_{n=1}^{2E} a_i^{(n)}\overline{a_j^{(n)}}\,\mathrm{d}\vec{\kappa} = 0, \tag{4.14}$$

where the last equality follows since the eigenvectors $\vec{a}^{(n)}$ of the matrix $S\mathrm{e}^{\mathrm{i}\boldsymbol{\kappa}}$ are orthogonal (so the integrand itself in fact vanishes identically). □

Proof of Theorem 1.4. We note that Theorem 1.4 is stated for L^2 normalized eigenfunctions. We have already calculated (see denominator in (3.7)) that the L^2 norm of an eigenfunction is

$$\left\|f_n\right\|^2 = \sum_{e=1}^{E}\left[\ell_e\left(\left|(a_e)_n\right|^2+\left|(a_{\hat{e}})_n\right|^2\right)+O\left(\frac{1}{k_n}\right)\right]. \tag{4.15}$$

Since terms of the form $O\left(\frac{1}{k_n}\right)$ do not affect the Cesàro mean, we get that Lemmas 4.2 and 4.3 prove exactly the expressions (1.10) and (1.11) in the Theorem. We proceed to prove the local Weyl law, (1.1).

Take $j\in\mathcal{E}$ to be an edge connected to the vertex v. We start by employing the expression for $\left|f_n(v)\right|^2$ which was already computed in the proof of Lemma 3.1 (see (3.7)).

$$\left\langle\left|f(v)\right|^2\right\rangle_n = \left\langle\frac{\left|a_j+a_{\hat{j}}\mathrm{e}^{\mathrm{i}k_n\ell_j}\right|^2}{\sum_{e=1}^{E}\left[\ell_e\left(\left|a_e\right|^2+\left|a_{\hat{e}}\right|^2\right)+O\left(\frac{1}{k_n}\right)\right]}\right\rangle_n \tag{4.16}$$

$$= \left\langle\frac{\left|a_j+a_{\hat{j}}\mathrm{e}^{\mathrm{i}k_n\ell_j}\right|^2}{\sum_{e=1}^{E}\ell_e\left(\left|a_e\right|^2+\left|a_{\hat{e}}\right|^2\right)}\right\rangle_n \tag{4.17}$$

$$= \left\langle\frac{\left|a_j\right|^2+\left|a_{\hat{j}}\right|^2}{\sum_{e=1}^{E}\ell_e\left(\left|a_e\right|^2+\left|a_{\hat{e}}\right|^2\right)}\right\rangle_n + 2\left\langle\frac{Re\left(\mathrm{e}^{\mathrm{i}k_n\ell_j}a_{\hat{j}}\overline{a_j}\right)}{\sum_{e=1}^{E}\ell_e\left(\left|a_e\right|^2+\left|a_{\hat{e}}\right|^2\right)}\right\rangle_n, \tag{4.18}$$

where going to the second line we omitted the term $O\left(\frac{1}{k_n}\right)$ in the Cesàro mean for the same reason as above. By Lemma 4.2, the first term in (4.18) equals $\frac{1}{|\Gamma|}$, and we proceed to evaluate the second term. From $(\vec{a})_n\in\ker\left(I-S\mathrm{e}^{\mathrm{i}k_nL}\right)$ and the expression for S in (2.5), we get that

$$(a_j)_n = \mathrm{e}^{\mathrm{i}k_n\ell_j}\sum_{i=1}^{\deg(v)}\left(\frac{2}{\deg(v)}-\delta_{ji}\right)(a_{\hat{i}})_n. \tag{4.19}$$

Thus:

$$\left\langle \frac{Re\left(\mathrm{e}^{\mathrm{i}k_n\ell_j}a_{\hat{j}}\overline{a_j}\right)}{\sum_{e=1}^{E}\ell_e\left(|a_e|^2+|a_{\hat{e}}|^2\right)}\right\rangle_n = \left(\frac{2}{\deg(v)}-1\right)\left\langle \frac{\left|a_{\hat{j}}\right|^2}{\sum_{e=1}^{E}\ell_e\left(|a_e|^2+|a_{\hat{e}}|^2\right)}\right\rangle_n \tag{4.20}$$

$$+\frac{2}{\deg(v)}\sum_{i\neq j\in\mathcal{E}_v} Re\left\langle \frac{a_{\hat{j}}\overline{a_{\hat{i}}}}{\sum_{e=1}^{E}\ell_e\left(|a_e|^2+|a_{\hat{e}}|^2\right)}\right\rangle_n . \tag{4.21}$$

By Lemmas 4.2 and 4.3, the first term is equal to $\frac{1}{2|\Gamma|}\left(\frac{2}{\deg(v)}-1\right)$, while the second term is equal to zero. Plugging this into (4.18), we obtain:

$$\left\langle |f(v)|^2\right\rangle_n = \frac{1}{|\Gamma|}+\frac{1}{|\Gamma|}\left(\frac{2}{\deg(v)}-1\right)=\frac{2}{\deg(v)|\Gamma|}. \tag{4.22}$$

□

5. Proof and discussion of Theorem 1.8 and Proposition 1.11

Proof of Theorem 1.8. As in the preceding proofs, we may consider the case of a single Robin vertex parameterized such that v is located at $x=0$. Using arguments similar to the ones used to derive (3.6) within the proof of Theorem 1.3, one can show that

$$\lim_{N\to\infty}\frac{\#\left\{n\leq N: d_n(\sigma)\leq x\right\}}{N}=\lim_{N\to\infty}\frac{\#\left\{n\leq N:\sigma\left|f_n^{(0)}(0)\right|^2\leq x\right\}}{N}. \tag{5.1}$$

Motivated by (4.17) in the proof of Theorem 1.4, we consider the following auxiliary function on Σ^{reg}:

$$g(\vec{\kappa}):=\frac{\left|a_j+a_{\hat{j}}\mathrm{e}^{\mathrm{i}\kappa_j}\right|^2}{\sum_{e=1}^{E}\ell_e\left(|a_e|^2+|a_{\hat{e}}|^2\right)}. \tag{5.2}$$

Denoting $\vec{\kappa}_n:=k_n\vec{\ell}$, we have that

$$\lim_{N\to\infty}\frac{\#\left\{n\leq N:\sigma\left|f_n^{(0)}(0)\right|^2\leq x\right\}}{N}=\lim_{N\to\infty}\frac{\#\left\{n\leq N:\sigma g(\vec{\kappa}_n)\leq x\right\}}{N}. \tag{5.3}$$

For a fixed $x\in\mathbb{R}$, define the following characteristic function on Σ^{reg}:

$$\eta_x(\vec{\kappa})=\begin{cases}1 & g(\vec{\kappa})\leq\frac{x}{\sigma}\\ 0 & \text{Otherwise}\end{cases} \tag{5.4}$$

We claim that $\eta_x(\vec{\kappa})$ is Riemann integrable for every $x\in\mathbb{R}$. As in the proof of Lemma 4.2, we employ the proof of lemma 4.25 in [2] to get that all functions of the form $|a_j(\vec{\kappa})|^2$ and , $a_j(\vec{\kappa})\overline{a_{\hat{j}}}(\vec{\kappa})$ are real analytic functions on Σ^{reg}. Since the denominator in (5.2) is bounded from below by a positive value, we conclude that g is real analytic as well. We get by [3, lem. 7.1] that for each connected component $\mathcal{M}$ of Σ^{reg}, either g is constant or its level sets are of measure zero. In particular, either the sublevel set $\left\{g(\vec{\kappa})\leq\frac{x}{\sigma}\right\}\cap\mathcal{M}$ is $\mathcal{M}$ or it is a submanifold of $\mathcal{M}$. In both cases it has a boundary of measure zero. This implies that $\eta_x(\vec{\kappa})$ is indeed Riemann integrable for every x.

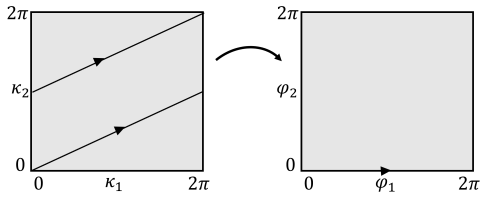

FIGURE 5.1. The torus flow $\phi(k) = (2k, k)$ on $\mathbb{T}^2$ as an example of rationally dependent entries (here $D = 1$). After the change of coordinates $(\varphi_1, \varphi_2) = \frac{1}{3}(\kappa_1 + \kappa_2, \kappa_1 - 2\kappa_2)$, we get the flow $\tilde{\phi}(k) = (k, 0)$, which is dense in the first component and constant in the second component.

The Riemann integrability of $\eta_x(\vec{\kappa})$ allows to apply the ergodic theorem if we assume that the graph edge lengths are linearly independent over $\mathbb{Q}$. We proceed by first making this assumption (which is lifted later), and apply (5.1),(5.3) and Theorem 2.7 to obtain

$$F_\sigma(x) = \lim_{N\to\infty} \frac{\#\{n \le N : d_n(\sigma) \le x\}}{N} = \lim_{N\to\infty} \frac{\#\{n \le N : \sigma g(\vec{\kappa}_n) \le x\}}{N} \tag{5.5}$$

$$= \lim_{N\to\infty} \frac{1}{N}\sum_{n=1}^{N} \eta_x(\vec{\kappa}_n) = \int_{\Sigma^{\mathrm{reg}}} \eta_x(\vec{\kappa})\, d\mu_{\vec{\ell}} = \mu_{\vec{\ell}}\left(\vec{\kappa} : g(\vec{\kappa}) \le \frac{x}{\sigma}\right). \tag{5.6}$$

We thus see that $F_\sigma(x)$ in fact returns the Barra-Gaspard measure of the sublevel sets of g. The fact that F_σ is a cumulative distribution function follows from $F_\sigma(x) = \mu_{\vec{\ell}}\left(\vec{\kappa} : g(\vec{\kappa}) \le \frac{x}{\sigma}\right)$. Moreover, Theorem 1.7 shows that the associated probability measure μ_σ must be supported on $\left[0, \frac{4\sigma}{\ell_{\min}}\right]$.

Now, we lift the assumption that the graph edge lengths are linearly independent over $\mathbb{Q}$. If the edge lengths are linearly dependent, then the associated torus flow (as defined Section 2.3) is no longer dense. Denoting the dimension of $\mathrm{span}_{\mathbb{Q}}\{\ell_e\}_{e\in\mathcal{E}}$ by D, we see that the torus flow is in fact only dense in a D-dimensional subtorus of the E-dimensional torus. By applying an appropriate change of coordinates, we may assume that the torus flow is dense when projected onto the first D coordinates of the torus, and constant when projected onto the last $E - D$ coordinates (see Figure 5.1). Hence, we may consider the flow within this D-dimensional subtorus. Repeating the same arguments as before, now considering the restriction of the function g to the intersection of Σ^{reg} and the subtorus, leads to the same conclusion – that F_σ is a cumulative distribution function.

Lastly, we consider the case where $\ell_e/\ell_{e'} \in \mathbb{Q}$, for all $e, e' \in \mathcal{E}$. In this case, $D = 1$ and the subtorus mentioned above is one-dimensional (see also Figure 5.1). Hence, the intersection of Σ^{reg} and the subtorus consists of only finitely many points. In particular the sequence $(g(\vec{\kappa}_n))_{n=1}^{\infty}$ contains finitely many values (it is in fact also periodic). This implies that $F_\sigma(x)$ only attains finitely many values, and so the associated measure μ_σ is a convex combination of Dirac masses. □

Remark 5.1. We conjecture that if not all ratios of edge lengths are rational, then the measure μ_σ is absolutely continuous with respect to the Lebesgue measure. We briefly explain the intuition behind this conjecture. Assuming that the function g from the proof above only attains regular values, then the co-area formula gives

$$F_\sigma(x) = \mu_{\vec{\ell}}\left(\vec{\kappa} : g(\vec{\kappa}) \le \frac{x}{\sigma}\right) = \int_{-\infty}^{x/\sigma} dt \int_{\{g=t\}} \frac{1}{|\nabla g|} d\mu_{\vec{\ell}}^t(\vec{\kappa}), \tag{5.7}$$

where $d\mu_{\vec{\ell}}^t$ denotes the surface area element of the Barra-Gaspard measure $\mu_{\vec{\ell}}$ on the level set $\{g = t\}$. Since F_σ can be expressed as an integral with respect to the Barra-Gaspard measure, which is absolutely continuous with respect to the Lebesgue measure, we see that μ_σ is as well.

This computation can be carried out assuming that ∇g does not vanish identically on some open subset of a level set. Since the function g is real analytic, this can happen only if g is constant on a whole connected component of Σ^{reg}. Hence, absolute continuity holds assuming that g is not constant on a connected component of Σ^{reg}. Nevertheless, the assumption that g is not constant on a connected component of Σ^{reg} is not proven here. This assumption is based on the intuition that such a constraint on g (and in turn on the values of $\vec{a}(\vec{\kappa})$) is too restrictive and on numerical experiments (see for example Figure 7.2 which suggests that μ_σ is indeed absolutely continuous). Finally, we refer the reader to a conjecture of a similar spirit in [3, rem. 7.2].

Proof of Proposition 1.11. This proof once again uses the function $g(\vec{\kappa})$ from the proof of Theorem 1.8.

Assume first that the graph's edge lengths are linearly independent over $\mathbb{Q}$, and so the torus flow considered in Section 2.3 is dense. Recall that the intersections of the torus flow with Σ^{reg} is exactly $(\vec{\kappa}_n)_{n=1}^\infty$. Since g is continuous on Σ^{reg} and the torus flow is dense, then for every value $c \in \overline{Im(g)}$, there exists a subsequence $g(\vec{\kappa}_{n_m})$ along the torus flow such that $g(\vec{\kappa}_{n_m}) \to c$. In order to connect the RNG with the values of g, we proceed exactly as in the proof of Theorem 1.8. Namely, combining (3.6) within the proof of Theorem 1.3 together with (4.17) in the proof of Theorem 1.4 gives that

$$\lim_{m\to\infty} d_{n_m}(\sigma) = \lim_{m\to\infty} \sigma \cdot g(\vec{\kappa}_{n_m}) = c\sigma, \tag{5.8}$$

and that this convergence is uniform in σ. These are the only possible accumulation points for the RNG, since the arguments above also show that any accumulation point must belong to $\overline{\{\sigma \cdot g(\vec{\kappa}_n)\}_{n=1}^\infty} = \overline{\sigma \cdot g(\Sigma^{\text{reg}})}$. Since g is a bounded and continuous function on a space with finitely many connected components, $\overline{g(\Sigma^{\text{reg}})}$ is a finite collection of compact intervals. These intervals are of course independent of the edge lengths of the graph (since g was defined independently of them). This proves the statement under the assumption above (edge lengths are linearly independent over $\mathbb{Q}$).

Similar to the proof of Theorem 1.8, the rationally dependent case can be proven by projecting the torus flow to the appropriate subtorus where the flow is dense, and repeating the same argument. Note that unlike the rationally independent case, the possible limit points now depend on the subtorus to which we restrict the function g, which of course depends on the graph edge lengths.

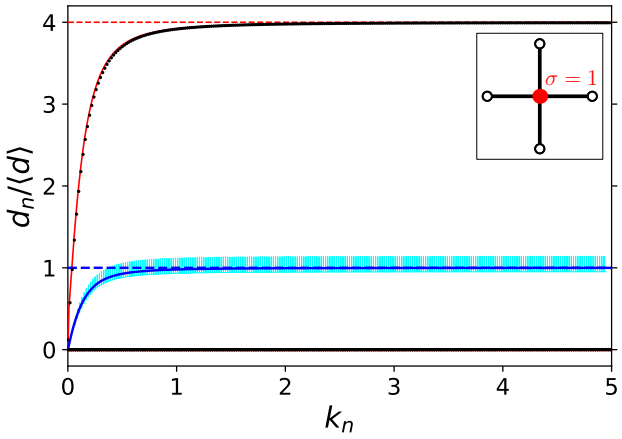

FIGURE 5.2. RNG (black points) for an equilateral star graph with Robin condition at the central vertex, scaled so that $\langle d \rangle_n = 1$ .The fluctuating light blue line is a running average and the blue lines on top of it are the analytic results from Equations (1.7), (A.12). The red dashed and full lines are the analytic bounds of Equation (1.14), (6.24). Since many of the states vanish at the central vertex, their corresponding RNG is zero. The RNG accumulates at two particular values, and does not get close to the mean value.

Lastly, in the degenerate case where $\ell_e/\ell_{e'} \in \mathbb{Q}, \forall e, e' \in \mathcal{E}$, the mentioned subtorus is one-dimensional (with a periodic flow along it), which implies that $\left(g\left(\vec{\kappa}_n\right)\right)_{n=1}^{\infty}$ attains only finitely many values. Hence, the set of accumulation points is finite and these are the degenerate intervals in the statement of the proposition. □

While Proposition 1.11 above shows the existence of converging subsequences for the RNG, it does not concretely specify the possible limit points. The proof of the proposition shows that that these limit points are determined by the possible values of the observable $|f_n(v)|^2$. We now discuss this briefly.

First, the discussion in Appendix C shows that zero is always an accumulation point for the RNG. This was proven for the case of a star graph in [20]. In the two-dimensional setting, [23] shows that under the assumption that the billiard dynamics associated with the domain is ergodic, there exists a subsequence of density 1 which converges pointwise to $\langle d \rangle_n(\sigma)$. The example of an equilateral star graph (Figure 5.2) shows that it is not true in general for graphs. We believe that under the assumption that the graph's edge lengths are linearly independent over $\mathbb{Q}$ (which is analogous to the ergodic billiards assumption made in [23]), then there does exist a subsequence which converges to the mean value. This is equivalent to stating that the support of the measure μ_σ from Theorem 1.8 contains the point $\langle d \rangle_n(\sigma)$. This was proven for a star graph in [20], and we can also prove this for graphs which contain loops, but the general case is still unclear. Even if such a subsequence exists, we believe that it cannot be of density 1 as in the two-dimensional setting. Indeed, if the measure μ_σ is absolutely continuous

in general (as we conjecture in Remark 5.1) then there is no converging subsequence of density 1.

6. Proof and Discussion of Theorem 1.7

6.1. **Proof of Theorem 1.7.** The main tool in the proof of Theorem 1.7 is the following lemma, which provides an upper bound for the eigenvalue derivatives with respect to the Robin parameter. This is done in terms of the star decomposition introduced before Theorem 1.7. Adding to those notations, we also denote

$$s_v := \frac{1}{\sum_{u\in\mathcal{U}_v} s_{v,u}^{-1}}, \tag{6.1}$$

so that s_v is the harmonic mean of the edge lengths of the star $\mathcal{S}_v$, divided by the number of edges in $\mathcal{S}_v$. If an auxiliary vertex coincides with a graph vertex such that $s_{v,u}=0$, then $s_v=0$.

Lemma 6.1. *For any star decomposition of* Γ *and any eigenvalue* $\lambda_n(\sigma)>0$ *,*

$$0 \le \frac{\mathrm{d}\lambda_n(\sigma)}{\mathrm{d}\sigma} \le 2\max_{v\in\mathcal{V}_\mathcal{R}} \left(|\mathcal{S}_v| + \frac{\sigma^2 s_v+\sigma}{\lambda_n(\sigma)} \right)^{-1}. \tag{6.2}$$

For the lowest eigenvalue $\lambda_1(0)=0$ *at* $\sigma=0$*, the following holds:*

$$\frac{\mathrm{d}\lambda_1(\sigma)}{\mathrm{d}\sigma}\Big|_{\sigma=0} = \frac{|\mathcal{V}_\mathcal{R}|}{|\Gamma|}. \tag{6.3}$$

Proof. The lower bound holds trivially by Lemma 2.1:

$$\frac{\mathrm{d}\lambda_n(\sigma)}{\mathrm{d}\sigma} = \sum_{v\in\mathcal{V}_\mathcal{R}} |f_n^{(\sigma)}(v)|^2 \ge 0. \tag{6.4}$$

For $\lambda_1(0)$, the corresponding eigenfunction is constant, and normalization implies that $\left|f_1^{(0)}(v)\right|^2 = \frac{1}{|\Gamma|}$ for all v, leading to (6.3).

To prove the upper bound, we fix an eigenvalue $\lambda_n(\sigma)>0$, and denote it by λ for brevity. On an edge $e=\{v,v'\}$, the corresponding eigenfunction can be written as

$$f|_e(x_e) = A_e\cos(kx_e-\varphi_{e,v}), \tag{6.5}$$

where x_e is the distance from v. Alternatively, using $x'_e := \ell_e - x_e$ and $\varphi_{e,v'} := k\ell_e - \varphi_{e,v}$, one can write

$$f|_e(x'_e) = A_e\cos(kx'_e-\varphi_{e,v'}). \tag{6.6}$$

The following relations then hold:

$$f(v) = A_e\cos\varphi_{e,v} \qquad \frac{\mathrm{d}\,f|_e}{\mathrm{d}x_e}\Big|_{x_e=0} = kA_e\sin\varphi_{e,v} \tag{6.7}$$

$$f(v') = A_e\cos\varphi_{e,v'} \qquad \frac{\mathrm{d}\,f|_e}{\mathrm{d}x'_e}\Big|_{x'_e=0} = kA_e\sin\varphi_{e,v'}, \tag{6.8}$$

and straightforward integration yields

$$\int_0^{\ell_e} (f|_e)^2(x)\,\mathrm{d}x_e = \frac{A_e^2}{2}\ell_e + A_e^2\frac{\sin\varphi_{e,v}\cos\varphi_{e,v}+\sin\varphi_{e,v'}\cos\varphi_{e,v'}}{2k}. \tag{6.9}$$

Using $\|f\|_{L^2}=1$ and denoting the set of edges connected to v by $\mathcal{E}_v$ as in Subsection 1.1, we have that

$$1 = \sum_{e\in\mathcal{E}}\int_0^{\ell_e}(f|_e)^2(x_e)\,\mathrm{d}x_e \tag{6.10}$$

$$= \sum_{e\in\mathcal{E}}\frac{A_e^2}{2}\ell_e + \sum_{e\in\mathcal{E}}A_e^2\frac{\sin\varphi_{e,v}\cos\varphi_{e,v}+\sin\varphi_{e,v'}\cos\varphi_{e,v'}}{2k} \tag{6.11}$$

$$= \sum_{e\in\mathcal{E}}\frac{1}{2}A_e^2(s_{v,u_e}+s_{v',u_e}) + \sum_{v\in\mathcal{V}}\sum_{e\in\mathcal{E}_v}A_e^2\frac{\sin\varphi_{e,v}\cos\varphi_{e,v}}{2k} \tag{6.12}$$

$$= \sum_{v\in\mathcal{V}}\sum_{e\in\mathcal{E}_v}\frac{1}{2}A_e^2 s_{v,u_e} + \sum_{v\in\mathcal{V}}\sum_{e\in\mathcal{E}_v}A_e^2\frac{\sin\varphi_{e,v}\cos\varphi_{e,v}}{2k}, \tag{6.13}$$

where in the first term of (6.12) we used $\ell_e = s_{v,u_e}+s_{v',u_e}$, which holds for any position of the auxiliary vertex u_e. We would like to replace the amplitudes A_e with the expressions from (6.7). This can be done whenever $\cos\varphi_{e,v}\neq 0$. Since the case $\cos\varphi_{e,v}=0$ implies $f(v)=0$, then dropping the (non-negative) terms with $f(v)=0$ gives the following inequality:

$$1 \geq \sum_{v\in\mathcal{V}:f(v)\neq 0}\frac{|f(v)|^2}{2}\sum_{e\in\mathcal{E}_v}\frac{s_{v,u_e}}{\cos^2\varphi_{e,v}} + \sum_{v\in\mathcal{V}}\frac{f(v)}{2k^2}\sum_{e\in\mathcal{E}_v}\frac{\mathrm{d}f_e}{\mathrm{d}x_e}\Big|_{x_e=0} \tag{6.14}$$

$$= \sum_{v\in\mathcal{V}_\mathcal{R}}\frac{|f(v)|^2}{2}\left(|\mathcal{S}_v| + \sum_{e\in\mathcal{E}_v}s_{v,u_e}\tan^2\varphi_{e,v} + \frac{\sigma}{k^2}\right), \tag{6.15}$$

where we have used the Robin condition (1.4) at v, dropped the (non-negative) terms corresponding to $v\notin\mathcal{V}_\mathcal{R}$, and replaced $\cos^{-2}\varphi_{e,v} = 1+\tan^2\varphi_{e,v}$.

We wish to estimate the second term in Equation (6.15). For $f(v)\neq 0$, we substitute (6.7) into the Robin condition (1.4) and find that

$$\forall v : f(v)\neq 0,\quad \sum_{e\in\mathcal{E}_v}\tan\varphi_{e,v} = \frac{\sigma}{k}. \tag{6.16}$$

Optimizing the second term in (6.15) in the variables $\varphi_{e,v}$ under the constraint (6.16), one obtains the following lower bound:

$$\sum_{e\in\mathcal{E}_v}s_{v,u_e}\tan^2\varphi_{e,v} \geq \frac{\sigma^2}{k^2}s_v, \tag{6.17}$$

where s_v is defined in (6.1). The lower bound in (6.17) is attained by

$$\forall e\in\mathcal{E}_v,\quad \tan\varphi_{v,e} = \frac{1}{s_{v,u_e}}\cdot\frac{\sigma}{k}s_v. \tag{6.18}$$

Substituting (6.17) in (6.15) we get:

$$1 \geq \sum_{v\in\mathcal{V}_{\mathcal{R}}} \frac{|f(v)|^2}{2}\left(|\mathcal{S}_v| + \frac{\sigma^2 s_v + \sigma}{k^2}\right) \tag{6.19}$$

$$\geq \min_{v\in\mathcal{V}_{\mathcal{R}}}\left(|\mathcal{S}_v| + \frac{\sigma^2 s_v + \sigma}{k^2}\right)\sum_{v\in\mathcal{V}_{\mathcal{R}}} \frac{|f(v)|^2}{2}. \tag{6.20}$$

Substituting this in (6.4) provides the required upper bound in the lemma. □

The proof of Theorem 1.7 is now straightforward.

Proof. Integrating over the bounds from (6.2) gives

$$0 \leq d_n(\sigma) \leq \int_0^\sigma 2\max_{v\in\mathcal{V}_{\mathcal{R}}}\left(|\mathcal{S}_v| + \frac{s_v t^2 + t}{\lambda_n(t)}\right)^{-1} \mathrm{d}t. \tag{6.21}$$

To get the bounds (1.14) in the theorem, we drop the second term in the expression above (which is positive). The inequality (1.15) follows since there always exists a star decomposition which contains only stars whose total length is at least $\frac{\ell_{\min}}{2}$; This star decomposition is obtained by taking u_e as the middle point of e for all edges $e \in \mathcal{E}$. □

Remark 6.2. A discussion of the optimality of the bounds is given in appendix C.

6.2. **Improved upper bound for the RNG.** We present here a better bound than the one given in Theorem 1.7.

Fix $\sigma > 0$. For every $t \in [0,\sigma]$ choose a star decomposition, and denote by $v_t \in \mathcal{V}_{\mathcal{R}}$ the vertex which is selected by the max-condition in (6.2),

$$\max_{v\in\mathcal{V}_{\mathcal{R}}}\left(|\mathcal{S}_v| + \frac{t^2 s_v + t}{\lambda_n(t)}\right)^{-1}. \tag{6.22}$$

Fix the parameters $\check{s}, \check{S}$ such that

$$\forall t \in [0,\sigma], \quad |\mathcal{S}_{v_t}| \geq \check{S}, \qquad s_{v_t} \geq \check{s}. \tag{6.23}$$

For the purpose of getting a finer upper bound on the RNG, we will be interested to take the highest possible values for $\check{s}, \check{S}$. In particular, the bound in the next proposition will be valid only if $\check{s}, \check{S}$ are positive. We demonstrate that this can be achieved in the following two cases:

(i) For a star graph with Robin condition at the central vertex. The auxiliary vertices may be chosen to be the boundary vertices of the graph. Thus, the (degenerate) stars around these vertices have zero length. Since the boundary vertices are imposed with the Neumann-Kirchhoff condition, it is easy to see that v_t is not one of the boundary vertices. Hence, we may choose $\check{S}$ to be the total length of the graph, and $\check{s}$ to be the harmonic mean of its edge lengths divided by the degree. Indeed, both are non-zero.

(ii) Let the graph be arbitrary, with the same star decomposition fixed for all $t \in [0,\sigma]$. Then one can take $\check{S}$ as the minimal length of a star around a Robin vertex in the partition and $\check{s}$ as the minimum value of s_v for a star in the partition. If none of the partition vertices are placed at $\mathcal{V}_{\mathcal{R}}$, then indeed both

$\check{S}$ and $\check{s}$ are non-zero. In general, the bound stated in the next proposition is tighter if $\check{S}, \check{s}$ are large, i.e. if the stars around the Robin vertices are large. Therefore, if there are edges which connect a Robin vertex $u \in \mathcal{V}_{\mathcal{R}}$ with a Neumann vertex $w \in \mathcal{V} \backslash \mathcal{V}_{\mathcal{R}}$, then to maximize the values of $|\mathcal{S}_v|$ and s_v, one should choose a star partition for which the auxiliary vertex should be placed at w, similarly to what was done in case (i).

Proposition 6.3. *For $\check{s}, \check{S}$ as above and $\lambda_n(0) > \frac{1}{4\check{s}\check{S}}$,*

$$d_n(\sigma) < \left(\frac{\exp\left(2\alpha \arctan\left(\frac{\alpha}{2} \cdot [1 + 2\check{s}\sigma]\right)\right)}{\exp\left(2\alpha \arctan\left(\frac{\alpha}{2}\right)\right)} - 1 \right) \cdot \lambda_n(0), \tag{6.24}$$

with

$$\alpha = \frac{2}{\sqrt{4\lambda_n(0)\,\check{s}\check{S} - 1}}. \tag{6.25}$$

Proof. From Equation (6.2) in Lemma 6.1, it follows that

$$\frac{d\lambda_n(t)}{dt} \leq \frac{2\lambda_n(t)}{|\mathcal{S}_{v_t}|\,\lambda_n(t) + s_{v_t}t^2 + t} \leq \frac{2\lambda_n(t)}{\check{S}\lambda_n(0) + \check{s}t^2 + t}. \tag{6.26}$$

Thus, $\lambda_n(\sigma)$ is bounded from above by the function $\lambda(\sigma)$ satisfying the differential equation

$$\frac{d\lambda}{dt} = \frac{2\lambda(t)}{A + 2Bt + Ct^2}, \tag{6.27}$$

with $A = \lambda_n(0)\,\check{S}$, $B = 1/2$, $C = \check{s}$ and initial condition $\lambda(0) = \lambda_n(0)$. Solution by separation of variables gives

$$\ln\frac{\lambda(\sigma)}{\lambda(0)} = \int_0^\sigma dt \frac{2}{A + 2Bt + Ct^2} = 2\alpha \arctan(\alpha[Ct + B])\Big|_0^\sigma \qquad (AC > B^2), \tag{6.28}$$

with $\alpha = (AC - B^2)^{-1/2}$ corresponding to (6.25).

Solving (6.28) above for $\lambda_n(\sigma) - \lambda_n(0)$ provides the given upper bound for $d_n(\sigma)$. Since equality holds in (6.26) only for $\lambda_n(t) = \lambda_n(0)$ (and then $d_n \equiv 0$), the inequality in (6.24) is strict.

□

Figures 1.2 and C.3(a) demonstrate the sensitivity and RNG values for a star graph with four edges and $\mathcal{V}_{\mathcal{R}}$ consisting of just the central vertex. In these figures, the solid red line was calculated with parameters as described in case (i) above. By Theorem 1.3, the limiting mean value of the RNG for this star graph is $\sigma/2|\Gamma|$, while from (1.14) with $|\mathcal{S}_v| = |\Gamma|$ we find that the upper bound is larger than the mean by a factor of $\deg(v_0) = 4$. Figures C.3(b) and 6.1 demonstrate the sensitivity and RNG values for a tetrahedron graph with $\mathcal{V}_{\mathcal{R}} = \mathcal{V}$. The optimal partition used to draw the bounds in these figures was found numerically. It has $|\mathcal{S}_v| = |\Gamma|/4$, i.e., all stars in the partition have the same total length. Once again, the ratio between the mean gap and upper bound is determined by the degree of the Robin vertices (3 in this case).

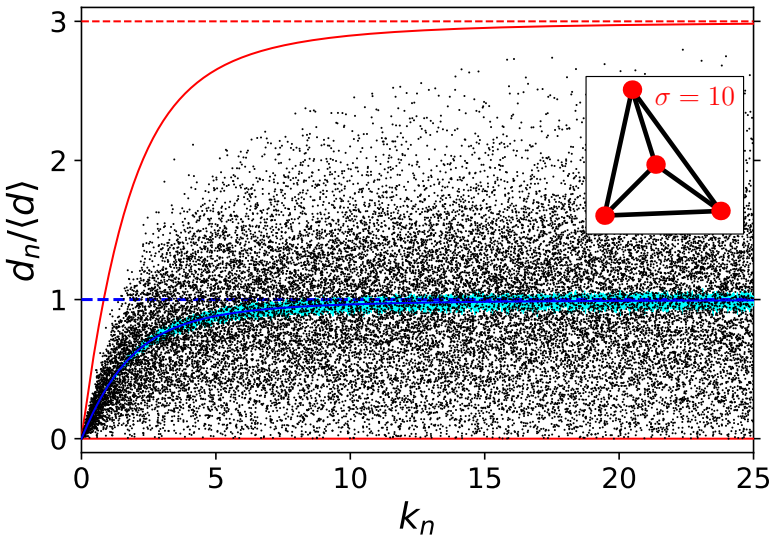

FIGURE 6.1. Scatter plot of the first 25,000 Robin-Neumann gaps for a tetrahedron with Robin condition at all vertices, scaled so that $\langle d \rangle_n(\sigma) = 1$. The light blue line is a running average and the blue lines on top of it are the results from (1.7), (A.12). The red dashed and full lines are the bounds from (1.14), (6.24).

7. Discussion and open questions

We conclude this work by comparing its results to the ones presented in [20, 21, 23] and raising several open questions.

Limiting mean value. Theorem 1.3 states that the mean value of the RNG is given by the following expression:

$$\langle d \rangle_n(\sigma) = \frac{2\sigma}{|\Gamma|} \sum_{v \in \mathcal{V}_{\mathcal{R}}} \frac{1}{\deg(v)}. \tag{7.1}$$

This expression bears obvious similarity to the result introduced in [23] for planar domains

$$\langle d \rangle_n(\sigma) = \frac{2|\partial\Omega|}{|\Omega|}\sigma, \tag{7.2}$$

which is also the expression proven in [21] for the hemisphere.

In the graph setting, the boundary term $|\partial\Omega|$ is replaced by a discrete measure on the set of Robin points. Interestingly, this discrete measure assigns to each vertex a total weight which is inversely proportional to its degree. Heuristically, if a vertex "meets" the graph from many different sides, then it is less likely to "feel" the Robin perturbation.

While this property is seemingly unique for the graph setting, we believe that at least in a sense, a similar effect also exists for two-dimensional domains. For instance, one can consider a domain with a two sided boundary (as in Figure 7.1) and replace the usual one-sided Robin condition $\frac{\partial f}{\partial n} + \sigma f = 0$ with the δ-transmission condition. This

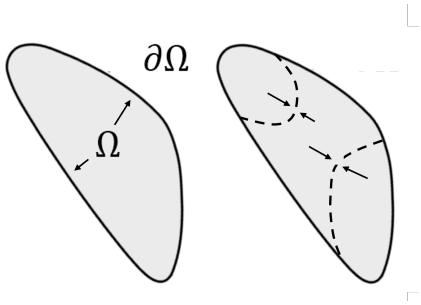

FIGURE 7.1. A one-sided boundary compared to a two-sided boundary.

condition consists of continuity of the function and a "two-sided" Robin condition:

$$\frac{\partial f_1}{\partial n_1} + \frac{\partial f_2}{\partial n_2} + \sigma f = 0. \tag{7.3}$$

In this case, we believe that the corresponding expression in (7.2) should be divided by two, whenever the two-sided boundary is considered. In this sense, the degree of the vertex can be replaced by the number of sides of the boundary which are in contact with the domain. This idea is further developed in [11], where the notion of circumference for a quantum graph is introduced.

Bounds. The uniform boundedness of the Robin-Neumann gaps in σ proven in Proposition 1.6 and Theorem 1.7 agrees with the result proven for star graphs in [20]. Having uniform bounds on the gaps is interesting, since this does not always hold when one passes to the two-dimensional setting. While the sequence of RNG is bounded for some domains (with explicit bounds for the rectangle given in [22]), the sequence is known to be unbounded for the hemisphere. It is also conjectured to be unbounded for certain planar domains, like the disk.

RNG distribution and its higher moments. Theorem 1.8 and Proposition 1.11 provide information about the distribution of the RNG, which is governed by a probability distribution similar to the one discussed in [20] (see e.g. Figure 7.2). A very natural question to ask is what else can be said about this probability distribution, and what other geometric information about the graph it holds.
Since the expectation of this probability measure can be computed explicitly (as in Theorem 1.3), it is sensible to try and study the measure μ_σ by computing the higher moments as well. Naively, the computation of the higher moments could be carried out by an approach similar to the one used in proving Theorem 1.3 – defining the higher moments as functions on the secular manifold, and then computing the corresponding integral. Yet, it turns out that the higher moments cannot be expressed as well defined functions on the secular manifold. Since this approach fails for the higher moments, this problem holds an additional challenge of finding a different way to perform the computation.

From Robin to other vertex conditions. Lastly, we address the possible generalization of the results to other vertex conditions. For instance, one may ask whether

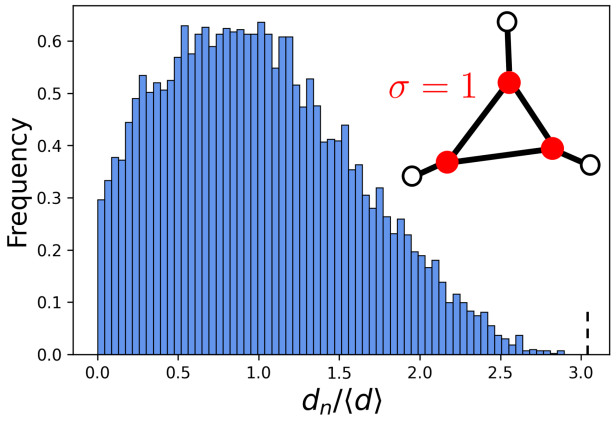

FIGURE 7.2. Histogram of the first 10,000 values of the RNG, normalized so that $\langle d_n \rangle (\sigma) = 1$. The Robin vertices are marked in red in the upper right corner. The frequencies are normalized so that the total area under the histogram is 1, indicating the possible probability distribution. An estimate for the upper bound appearing in (1.14) is marked by a dashed vertical line.

similar results can be obtained for the counterpart δ'-type condition (see e.g. [1, 6]). In this case, the eigenvalue curves are non-increasing with the coupling parameter σ, and one can similarly define the family of gaps.

From numerical exploration, it seems that if one defines

$$\tilde{d}_n (\sigma) := \lambda_n (0) - \lambda_n (\sigma) = k_n^2 (0) - k_n^2 (\sigma) , \tag{7.4}$$

then the given sequence is no longer bounded, and its mean value does not converge. This suggests that generalization of the results above to other vertex conditions might not always be possible. Interestingly, if one instead defines

$$\tilde{d}_n (\sigma) = k_n (0) - k_n (\sigma) , \tag{7.5}$$

then the given sequence does seem to be bounded, and the mean value converges as before (see Figure 7.3), although it is not clear to us at this point what it converges to.

When trying to repeat the computation of the mean value of gaps for the δ' condition, one comes across a problem similar to the one with the higher moments. It turns out that it is not possible to define the corresponding gap as a function on the secular manifold, which makes it difficult to apply the approach presented in this work. It is possible that the computation may be done using the local Weyl law proven in [11] for general vertex conditions. But as the numerical example above suggests, the results might be very different.

Acknowledgement. We are indebted to Uzy Smilansky for gluing our team together. Uzy participated in many discussions towards the formation of this paper. He provided ideas which stimulated the scientific content and promoted our work process. We are grateful to him for all that.

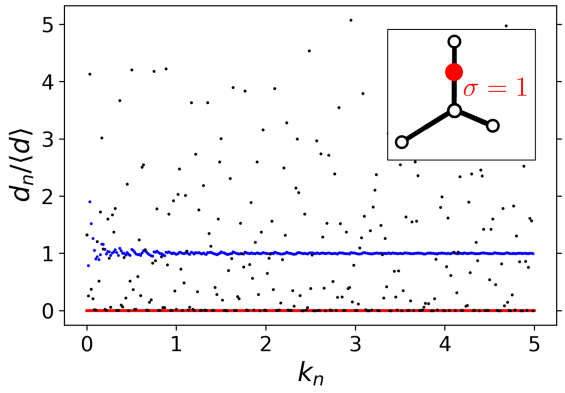

FIGURE 7.3. The first three-hundred values of the spectral gap for the δ' condition on a star graph (red points). The mean value of the sequence up to the n^{th} eigenvalue is indicated by blue points and suggests that it converges (namely, the Cesàro mean exists). The plot also suggests that the sequence is bounded.

We thank Nadav Yesha for a very clear presentation of the analogous results on manifolds, which encouraged us to start this work. This work also gained from interesting discussions and email correspondence with Lior Alon, Gregory Berkolaiko, James Kennedy and Zeev Rudnick, and we thank them for that. We also thank the referees for detailed feedback which helped improve the paper. GS thanks the Institute of Mathematics at the University of Potsdam, where some of this work as been done.

RB and GS were supported by ISF (Grant No. 844/19) and by the Binational Science Foundation Grant (Grant No. 2016281).

APPENDIX A. AN ADDITIONAL APPROACH FOR DERIVING THE MEAN ROBIN-NEUMANN GAP

In this appendix, we present an alternative derivation for the mean value of the Robin-Neumann gap. This is done by considering a so-called "local average" of the RNG with respect to the wave number k (instead of averaging with respect to n). This approach is not as rigorous as the proof of Theorem 1.3. Nevertheless, it is advantageous in that it provides not only the limiting mean value of the RNG, but also the running mean as it depends on k, see Figure 1.2.

We begin by considering the situation where the Robin condition is imposed at a single vertex, and later generalize to multiple vertices. In this case, we know that the eigenvalues interlace (see [8, thm. 3.1.8]); if $\sigma < \sigma'$, then for all $n \in \mathbb{N}$

$$k_n(\sigma) \leq k_n(\sigma') < k_{n+1}(\sigma). \tag{A.1}$$

This can be rewritten in terms of the number counting function $\mathcal{N}(k,\sigma) := |\{n \in \mathbb{N} : k_n \leq k\}|$. Mainly, this means that the spectral shift, which is the difference between the number counting functions at fixed k, may only take the values zero and one,

$$\Delta^{\sigma}\mathcal{N}(k) := \mathcal{N}(k,0) - \mathcal{N}(k,\sigma) \in \{0,1\}. \tag{A.2}$$

We denote the length of the intervals where the spectral shift is equal to one by

$$\delta_n(\sigma) := k_n(\sigma) - k_n(0). \tag{A.3}$$

Note that these intervals are defined similarly as the RNG, but for the difference between the k values rather than the eigenvalues.

By the Weyl law for metric graphs (see [8, 15]) for a fixed value of σ, the mean distance between consecutive values of $\{k_n(\sigma)\}$ is

$$\langle \Delta k \rangle := \pi / |\Gamma|. \tag{A.4}$$

Hence, for large $K > 0$, the interval $[k - K/2, k + K/2]$ contains on average $N := K/\langle \Delta k \rangle$ values from $\{k_n(\sigma)\}$. Thus, defining a local k-average, the spectral shift in k is equal to:

$$\overline{\Delta^\sigma \mathcal{N}}(k) = \frac{1}{K}\int_{k-K/2}^{k+K/2} \Delta\mathcal{N}^\sigma(k')\,dk' \approx \frac{|\Gamma|}{\pi}\cdot\frac{1}{N}\sum_{n=N_0+1}^{N_0+N}\delta_n(\sigma) = \frac{|\Gamma|\,\delta^\sigma(k)}{\pi}, \tag{A.5}$$

where $\{N_0+1,\ldots,N_0+N\}$ are the indices of the $\{k_n(\sigma)\}$ values which are contained in the interval $[k-K/2, k+K/2]$ (on average). Hence, $\delta^\sigma(k) := \frac{1}{N}\sum_{n=N_0+1}^{N_0+N}\delta_n(\sigma)$ is the mean spectral shift around k. The expression above holds up to an error of order N^{-1} due to the limits of the integration interval.

To evaluate the mean spectral shift above, we use the trace formula for the counting function (as derived in [16, 17]):

$$\mathcal{N}^\sigma(k,\sigma) = \frac{\Theta(k,\sigma)}{2\pi} + \frac{1}{\pi}\cdot Im\sum_{m=1}^{\infty}\frac{\mathrm{tr}U^m(k,\sigma)}{m}. \tag{A.6}$$

Here, $U(k,\sigma) := S^{(\sigma)}e^{ikL}$ is the unitary scattering matrix (as in Theorem 2.4) and $\Theta(k,\sigma) := \log(\det(U(k,\sigma)))$ is known as the total phase of $U(k,\sigma)$. Under the assumption that K is large enough (mainly, that $K \gg \pi/\ell_{\min}$, see [16, 17]), the contribution of the oscillatory term in (A.6) is suppressed by the averaging, and in leading order we have that

$$\overline{\Delta^\sigma \mathcal{N}}(k) = \frac{\overline{\Theta(k,0)} - \overline{\Theta(k,\sigma)}}{2\pi}. \tag{A.7}$$

The total phase was evaluated in [17] as

$$\Theta(k,\sigma) = 2k|\Gamma| - 2\sum_{v\in\mathcal{V}_\mathcal{R}}\arctan\left(\frac{\sigma}{\deg(v)\,k}\right). \tag{A.8}$$

Plugging this into (A.7) and then using (A.5) gives that for a single Robin vertex

$$\delta^\sigma(k) = \frac{1}{|\Gamma|}\arctan\left(\frac{\sigma}{\deg(v)\,k}\right). \tag{A.9}$$

Finally, we can define the k-averaged Robin-Neumann gap by

$$\langle d \rangle_k(\sigma) := (k + \delta^\sigma(k))^2 - k^2, \tag{A.10}$$

which under the assumption $\delta^\sigma(k) \ll k$, and together with (A.9), gives the following:

$$\langle d\rangle_k(\sigma) \approx 2k\delta^\sigma(k) = \frac{2k}{|\Gamma|}\arctan\left(\frac{\sigma}{\deg(v)\,k}\right). \tag{A.11}$$

For the more general case where the Robin condition is imposed at several vertices, we can repeat the same proof (applying the additivity of Equation (A.8)) to obtain

$$\langle d\rangle_k(\sigma) = \frac{2k}{|\Gamma|}\sum_{v\in\mathcal{V}_\mathcal{R}}\arctan\left(\frac{\sigma}{\deg(v)\,k}\right). \tag{A.12}$$

Note that for $k\to\infty$, one can recover the rigorously obtained expression from Theorem 1.3 by first order approximation of (A.12). On the other hand, for $k\to 0$ the average gap approaches zero. The average sensitivity of the gaps with respect to a change of the Robin parameter is obtained by differentiating (A.12) with respect to σ:

$$\left\langle\frac{d\lambda(\sigma)}{d\sigma}\right\rangle_n = \frac{2}{|\Gamma|}\sum_{v\in\mathcal{V}_\mathcal{R}}\frac{\lambda\deg(v)}{\sigma^2+\lambda\deg(v)^2} \tag{A.13}$$

$$\approx_{\lambda\to\infty}\frac{2}{|\Gamma|}\sum_{v\in\mathcal{V}_\mathcal{R}}\frac{1}{\deg(v)}. \tag{A.14}$$

A crucial assumption in the derivations above was that the averaging interval K contains many eigenvalues, which is required to neglect the oscillating terms in (A.6). At the same time, K must be small enough so that the value of (A.9) does not change by a large amount inside the given interval. Otherwise, the definition of a local average of the gap is not meaningful. The two conditions can only be met for graphs with a large metric length $|\Gamma|\to\infty$. Alternatively, one may employ an ensemble average over graphs where the topology is fixed and the edge lengths are varied. Having written the above, we refer to Figures 1.2, C.3 and 6.1, which demonstrate how close is (A.12) to a running mean value obtained by averaging over 21 adjacent eigenvalues.

Appendix B. Omitting the assumption of independence over $\mathbb{Q}$

Recall that in order to apply the ergodic theorem (Theorem 2.7), we added the assumption that the entries of the vector of edge lengths $\vec{\ell}$ are linearly independent over $\mathbb{Q}$. We now show that the results of Theorem 1.4 in fact hold without this assumption.

Proposition B.1. *Assumption 4.1 can be omitted in Theorem 1.4.*

Proof. We give the proof for the expression (1.8), where the proof of (1.10), (1.11) is similar. This is a simple denseness argument. Fix a discrete graph $G=(\mathcal{V},\mathcal{E})$ and $v\in\mathcal{V}$. Denote:

$$\mathbb{R}^E_+ = \left\{\vec{x}\in\mathbb{R}^E : x_i>0, \forall i\in\{1,..,E\}\right\}. \tag{B.1}$$

For $\vec{\ell}\in\mathbb{R}^E_+$, denote by $\Gamma_{\vec{\ell}}$ the metric graph obtained by assigning the vector of edge lengths $\vec{\ell}$ to the fixed combinatorial graph G.

Define the following function:

$$\phi_1 : \mathbb{R}_+^E \to \mathbb{R}^{\mathbb{N}}, \tag{B.2}$$

$$\phi_1\left(\vec{\ell}\right) = \left(\left|f_1^{\vec{\ell}}(v)\right|^2, \left|f_2^{\vec{\ell}}(v)\right|^2, ...\right), \tag{B.3}$$

where $f_n^{\vec{\ell}}$ is an n^{th} L^2 normalized eigenfunction for the metric graph $\Gamma_{\vec{\ell}}$ as in Theorem 1.4.

Denote by P the subset of $\mathbb{R}_+^E$ of vectors whose coordinates are rationally independent. This is a dense subset of $\mathbb{R}_+^E$. Denote the set of Cesàro summable sequences by $\mathcal{C}$. Define the following functions:

$$\phi_2 : \mathcal{C} \to \mathbb{R}, \tag{B.4}$$

$$\phi_2\left((c_n)_{n=1}^{\infty}\right) = \lim_{N\to\infty} \frac{1}{N} \sum_{n=1}^{N} c_n \tag{B.5}$$

$$\phi : P \to \mathbb{R}, \tag{B.6}$$

$$\phi = \phi_2 \circ \left(\phi_1|_P\right). \tag{B.7}$$

By the version we proved for Theorem 1.4, ϕ is a well defined function on P. For all $\vec{x} \in \mathbb{R}_+^E$, there exists a neighborhood $U \subset \mathbb{R}_+^E$ of $\vec{x}$, such that ϕ is uniformly continuous on $U \cap P$, since it is simply given by the expression:

$$\phi\left(\vec{\ell}\right) = \frac{2}{\deg(v) \sum_{e=1}^{E} \ell_e}. \tag{B.8}$$

Since P is dense in $\mathbb{R}_+^E$ and ϕ is locally uniformly continuous (in the sense mentioned above), it can be extended into a continuous function $\tilde{\phi}$ on $\mathbb{R}_+^E$.

To complete the proof, we should show that $\tilde{\phi} = \phi_2 \circ \phi_1$ and that $\tilde{\phi}$ is given by expression (B.8). This is based on standard topological arguments which we merely sketch here, and refer the interested reader to [26, prop. 5.16] for further details. First, one shows that ϕ_1 is continuous. From here follows $\phi_1\left(\mathbb{R}_+^E\right) \subset \mathcal{C}$, using that set of Cesàro summable sequences is closed. Now one gets that $\phi_2 \circ \phi_1$ is well defined and continuous, and concludes $\tilde{\phi} = \phi_2 \circ \phi_1$ since those functions agree on the dense set P. Finally, the continuity of $\tilde{\phi}$ implies that it is indeed given by (B.8) and completes the proof. □

Remark B.2. It is worth noting that while the limiting mean values in Theorems 1.3, 1.4 are the same for the rationally dependent case, the behavior of the sequences themselves might be drastically different in that case. For instance, for the case of an equilateral star graph, one can show that the sequence of RNG accumulates around two values, and does not get close to the mean value. Nevertheless, the Cesàro mean converges to its expected value as in Theorem 1.3. The above is nicely exemplified in Figure 5.2.

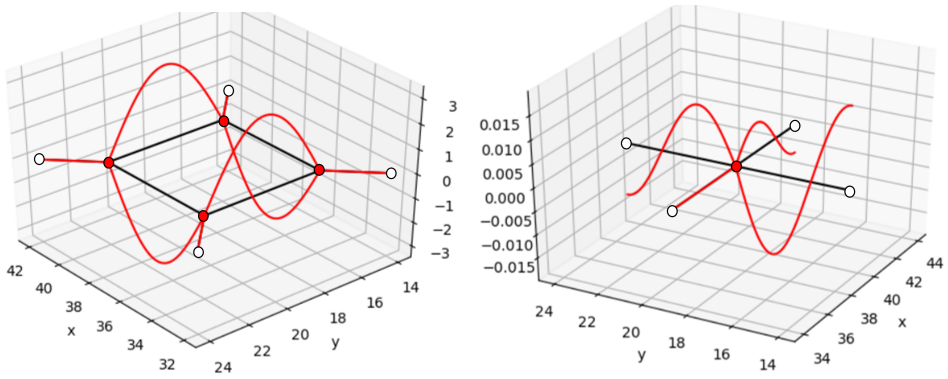

FIGURE C.1. Two examples of states with zero sensitivity: Case (i) of a graph with a cycle, where the Robin vertices are placed at the four vertices of the inner square. Case (ii) of a star graph with Robin condition at the central vertex. In both cases the eigenfunction vanishes at the set $\mathcal{V}_\mathcal{R}$, resulting in zero sensitivity, i.e., $\frac{\mathrm{d}\lambda_n}{\mathrm{d}\sigma}=0$ for all $\sigma \in \mathbb{R}$.

APPENDIX C. OPTIMALITY OF THE BOUNDS ON THE RNG

C.1. **Optimality of the lower bound in Lemma 6.1 and Theorem 1.7.** Under certain assumptions, the lower bound of zero in Lemma 6.1 and Theorem 1.7 is optimal. This happens when the corresponding graph allows for Robin eigenfunctions whose absolute values at the set $\mathcal{V}_\mathcal{R}$ are arbitrarily small. This results in very low sensitivity to the Robin condition (i.e., small value of $\frac{\mathrm{d}\lambda_n}{\mathrm{d}\sigma}$), giving an arbitrarily small value to the RNG. We demonstrate this for two typical cases:

(i) The graph contains a cycle.
(ii) The graph is a tree, where at least two leaves (denoted by v_1, v_2) are not contained in $\mathcal{V}_\mathcal{R}$.

For the graphs above, eigenfunctions with low sensitivity to the Robin condition exist. In the case where the edge lengths of the graph are linearly dependent over $\mathbb{Q}$ (rationally dependent), constructing such eigenfunctions is simple. In fact, one can construct eigenfunctions which vanish on the set $\mathcal{V}_\mathcal{R}$. By Lemma 2.1, these eigenfunctions have zero sensitivity to the Robin condition (i.e., $\frac{\mathrm{d}\lambda_n}{\mathrm{d}\sigma} = 0$ for all $\sigma \in \mathbb{R}$), and they thus give zero RNG – $d_n(\sigma) = 0$ for all $\sigma > 0$. We now point out the existence of these eigenfunctions (see also Figures C.1 and C.2).

In case (i), one can select a cycle on the graph, and choose the wave number k such that all edge lengths in the cycle are integer multiples of the wave length $\Lambda := 2\pi/k$. Under these conditions, there exist eigenfunctions which vanish on the entire graph apart from the given cycle. In particular, those eigenfunctions vanish at all vertices on the given cycle. In case (ii), consider the (unique) path connecting the vertices v_1, v_2. Then similar to before, one can choose edge lengths and k such that all edges in the path are integer multiples of Λ, with the exception of the edges adjacent to v_1, v_2, to which an additional $\Lambda/4$ is added. Under these conditions, there exist eigenfunctions which vanish on all of the graph apart from the given path. In particular, those eigenfunctions

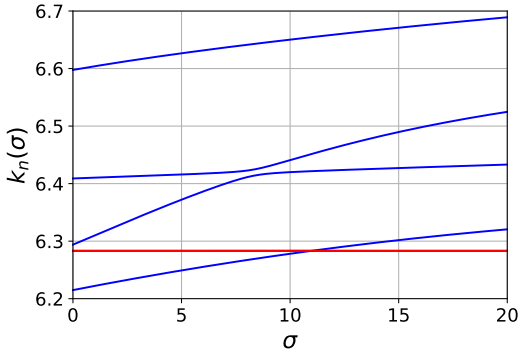

FIGURE C.2. The eigenvalue curves for a tetrahedron graph with $\mathcal{V}_\mathcal{R} = \mathcal{V}$. The horizontal red curve at $k = 2\pi$ corresponds to a state which is supported on a triangle subgraph and vanishes at all $v \in \mathcal{V}_\mathcal{R}$. This gives a state with zero sensitivity as in case (i), which results in $d_n(\sigma) = 0$.

vanish at all interior vertices along the given path, and their derivative at v_1, v_2 vanishes. All eigenfunctions described above (for both cases (i) and (ii)) vanish at $\mathcal{V}_\mathcal{R}$, as required.

While it is impossible to construct eigenfunctions with zero sensitivity in the general case of rationally independent edge lengths, one can still use the construction above to find eigenfunctions with arbitrarily small sensitivity. This can be done by approximating the given edge lengths with rationally dependent edge lengths, and then applying the method above. This will give a sequence of eigenfunctions whose value at $\mathcal{V}_\mathcal{R}$ is arbitrarily small, resulting in a subsequence of $d_n(\sigma)$ which tends to zero.

The frequency of such eigenfunctions with low sensitivity has been estimated in [24]. It depends on the number of edge lengths that determine the value of k in the construction above. For example, these eigenfunctions appear more frequently in Figure C.3 (a) than in (b). This is since in case (a) of a star graph the supporting path which determines k contains two edges, while in case (b) of a tetrahedron it contains three edges forming a cycle. The figures show that while the lower bound is not attained in these cases, it is still tight.

C.2. **Optimality of the upper bound in Lemma 6.1.** In order to construct eigenfunctions which attain the upper bound of Lemma 6.1, equality must hold in Equations (6.14), (6.18), (6.19) and (6.20). We provide two examples for specific graphs which satisfy this.

For the first example, consider an equilateral star graph with edges of length ℓ and Robin condition at the central vertex v_0. On each edge, the L^2 normalized eigenfunctions can be written as

$$f_e(x_e) = \frac{1}{\sqrt{\deg(v_0)\ell}} \cos(kx_e - \varphi_{e,v_0}), \tag{C.1}$$

where the edges are parameterized so that the central vertex v_0 corresponds to $x_e = 0$ for all e. Then by choosing $k > 0$ such that

$$\tan k\ell = \frac{\sigma}{k \deg(v_0)}, \tag{C.2}$$

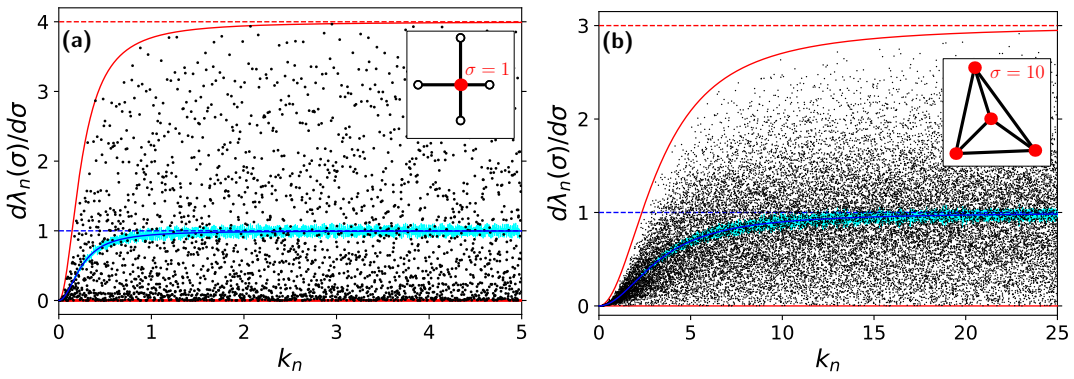

FIGURE C.3. Scatter plot of the eigenvalue sensitivities $\frac{d\lambda_n}{d\sigma}$ for (a) the star graph from Figure 1.2 and (b) the tetrahedron graph from Figure 6.1 below. The values are scaled so that the mean sensitivity is one. The light blue lines are running averages, and the blue lines on top of it are the analytic results from Equations (A.13),(A.14). The red lines are the upper bound of (6.2) with and without the second term, respectively.

and taking $\varphi_{e,v_0} = k\ell$, we get a valid Robin eigenfunction. Moreover, this eigenfunction does not vanish at any vertex, so equality holds in (6.14). Now, choose a trivial star decomposition, where the points u_e are located at the outer vertices. In this case, all terms in (6.14) which correspond to the outer vertices vanish. For the remaining vertex v_0, (6.18) is satisfied and equality holds in (6.19). This also gives equality in (6.20).

The assumption of equal edge lengths which was used for this construction can be relaxed. Similar to the previous subsection, choosing arbitrary edge lengths will lead to the existence of eigenfunctions with sensitivity arbitrarily close to the upper bound. However, since all edges of the graph are involved in the construction, the probability of such an eigenfunction is much lower than in the case of approaching the lower bound zero (where only a small subset of the edges were involved), see Figure C.3. Moreover, condition (C.2) which is used to determine k depends on σ and can be satisfied at most at isolated points along the integral in Equation (1.14). Therefore, unlike the lower bound zero, the upper bound in Theorem 1.7 cannot be realized by this construction.

The second construction is similar, but concerns a regular graph with no neighboring Neumann vertices. For this construction, one should take the length of edges connecting a Robin vertex to a Neumann vertex to be ℓ, and the length of an edge connecting two Robin vertices to be 2ℓ. Just as before, choose k according to (C.2) above and $\varphi_{e,v} = k\ell$ for all $v \in \mathcal{V}$. This will once again give a valid eigenfunction. Now, choose a star decomposition which is attained by splitting the edges which connect two Robin vertices in the middle. i.e, $s_{v,u_e} = \ell$ for all Robin vertices and $s_{v',u_e} = 0$ for all Neumann vertices. Then just as in the example above, the Neumann vertices have zero contribution to (6.14), while for the Robin vertices (6.18) holds and so there is equality in (6.19). Since all star graphs around Robin vertices are identical, equality holds in (6.20) as well.

References

[1] S. Albeverio, F. Gesztesy, R. Høegh-Krohn, and H. Holden. *Solvable models in quantum mechanics*. Texts and Monographs in Physics. Springer-Verlag, New York, 1988.

[2] L. Alon. *Quantum graphs - Generic eigenfunctions and their nodal count and Neumann count statistics*. PhD thesis, Mathamtics Department, Technion - Israel Institute of Technology, 2020.

[3] L. Alon and R. Band. Neumann domains on quantum graphs. *Annales Henri Poincaré*, 2021.

[4] L. Alon, R. Band, and G. Berkolaiko. Nodal statistics on quantum graphs. *Comm. Math. Phys.*, 2018.

[5] L. Alon, R. Band, and G. Berkolaiko. Universality of nodal count distribution in large metric graphs. *Experimental Mathematics*, 2022.

[6] J. E. Avron, P. Exner, and Y. Last. Periodic Schrödinger operators with large gaps and Wannier-Stark ladders. *Phys. Rev. Lett.*, 72(6):896–899, 1994.

[7] F. Barra and P. Gaspard. On the level spacing distribution in quantum graphs. *J. Statist. Phys.*, 101(1–2):283–319, 2000.

[8] G. Berkolaiko and P. Kuchment. Dependence of the spectrum of a quantum graph on vertex conditions and edge lengths. In *Spectral Geometry*, volume 84 of *Proceedings of Symposia in Pure Mathematics*. American Math. Soc., 2012. preprint `arXiv:1008.0369`.

[9] G. Berkolaiko and P. Kuchment. *Introduction to Quantum Graphs*, volume 186 of *Math. Surv. and Mon.* AMS, 2013.

[10] G. Berkolaiko and B. Winn. Relationship between scattering matrix and spectrum of quantum graphs. *Trans. Amer. Math. Soc.*, 362(12):6261–6277, 2010.

[11] P. Bifulco and J. Kerner. Comparing the spectrum of Schrödinger operators on quantum graphs. *arXiv:2212.13954*.

[12] J. Bolte and S. Endres. The trace formula for quantum graphs with general self adjoint boundary conditions. *Ann. Henri Poincaré*, 10(1):189–223, 2009.

[13] D. Borthwick, E. M. Harrell II, and K. Jones. The heat kernel on the diagonal for a compact metric graph. *Annales Henri Poincare*, 2022.

[14] Y. Colin de Verdière. Semi-classical measures on quantum graphs and the Gauß map of the determinant manifold. *Annales Henri Poincaré*, 16(2):347–364, 2015. also `arXiv:1311.5449`.

[15] S. Gnutzmann and U. Smilansky. Quantum graphs: Applications to quantum chaos and universal spectral statistics. *Adv. Phys.*, 55(5–6):527–625, 2006.

[16] T. Kottos and U. Smilansky. Quantum chaos on graphs. *Phys. Rev. Lett.*, 79(24):4794–4797, 1997.

[17] T. Kottos and U. Smilansky. Periodic orbit theory and spectral statistics for quantum graphs. *Ann. Physics*, 274(1):76–124, 1999.

[18] T. Kottos and U. Smilansky. Chaotic scattering on graphs. *Phys. Rev. Lett.*, 85(5):968–971, 2000.

[19] Y. Latushkin and S. Sukhtaiev. First-order asymptotic perturbation theory for extensions of symmetric operators. *arXiv:2012.00247*, 2023.

[20] G. Rivière and J. Royer. Spectrum of a non-selfadjoint quantum star graph. *J. Phys. A*, 53(49):495202, 2020.

[21] Z. Rudnick and I. Wigman. On the robin spectrum for the hemisphere. *Annales mathématiques du Québec*, 2021.

[22] Z. Rudnick and I. Wigman. The robin problem on rectangles. *J. Math. Phys. 62, 113503*, 2021.

[23] Z. Rudnick, I. Wigman, and N. Yesha. Differences between robin and neumann eigenvalues. *Commun. Math. Phys.*, 2021. `arXiv:2008.07400`.

[24] H. Schanz and T. Kottos. Scars on quantum networks ignore the lyapunov exponent. *Phys. Rev. Lett. 90*, 2003.

[25] M. Sieber, H. Primack, U. Smilansky, I. Ussishkin, and H. Schanz. Semiclassical quantization of billiards with mixed boundary conditions. *Journal of Physics A: Mathematical and General*, 28(17):5041, sep 1995.

[26] G. Sofer. Spectral curves of quantum graphs with δs type vertex conditions. Master's thesis, Technion - Israel Institute of Technology, 2022.

Ram Band
(i) Faculty of Mathematics
Technion – Israel Institute of Technology
32000 Haifa
Israel
(ii) Institut für Mathematik
Universität Potsdam
14476 Potsdam
Germany
e-mail: ramband@technion.ac.il

Holgar Schanz
Hochschule Magdeburg-Stendal
39114 Magdeburg
Germany
e-mail: holger.schanz@h2.de

Gilad Sofer
Faculty of Mathematics
Technion – Israel Institute of Technology
32000 Haifa
Israel
e-mail: gilad.sofer@campus.technion.ac.il